

The Discovery of Polo-like Kinase 4 Inhibitors: Design and Optimization of Spiro[cyclopropane-1,3'[3H]indol]-2'(1'H)-ones as Orally Bioavailable Antitumor Agents

Peter Brent Sampson, Yong Liu, Narendra Kumar Patel, Miklos Feher, Bryan Forrest, Sze-Wan Li, Louise Edwards, Radoslaw Laufer, Yunhui Lang, Fuqiang Ban, Donald E. Awrey, Guodong Mao, Olga Plotnikova, Genie Leung, Richard Hodgson, Jacqueline Mason, Xin Wei, Reza Kiarash, Erin Green, Wei Qui, Nickolay Y. Chirgadzhe, Tak W. Mak, Guohua Pan, and Henry W Pauls

J. Med. Chem., **Just Accepted Manuscript** • DOI: 10.1021/jm500537u • Publication Date (Web): 27 May 2014

Downloaded from <http://pubs.acs.org> on June 21, 2014

Just Accepted

"Just Accepted" manuscripts have been peer-reviewed and accepted for publication. They are posted online prior to technical editing, formatting for publication and author proofing. The American Chemical Society provides "Just Accepted" as a free service to the research community to expedite the dissemination of scientific material as soon as possible after acceptance. "Just Accepted" manuscripts appear in full in PDF format accompanied by an HTML abstract. "Just Accepted" manuscripts have been fully peer reviewed, but should not be considered the official version of record. They are accessible to all readers and citable by the Digital Object Identifier (DOI®). "Just Accepted" is an optional service offered to authors. Therefore, the "Just Accepted" Web site may not include all articles that will be published in the journal. After a manuscript is technically edited and formatted, it will be removed from the "Just Accepted" Web site and published as an ASAP article. Note that technical editing may introduce minor changes to the manuscript text and/or graphics which could affect content, and all legal disclaimers and ethical guidelines that apply to the journal pertain. ACS cannot be held responsible for errors or consequences arising from the use of information contained in these "Just Accepted" manuscripts.



1
2
3
4
5
6
7
8
9
10
11
12
13
14
15
16
17
18
19
20
21
22
23
24
25
26
27
28
29
30
31
32
33
34
35
36
37
38
39
40
41
42
43
44
45
46
47
48
49
50
51
52
53
54
55
56
57
58
59
60

	Qui, Wei; University of Toronto, Pharmacology and Toxicology Chirgadze, Nickolay; University of Toronto, Pharmacology and Toxicology Mak, Tak; University Health Network, Campbell Family Institute for Breast Cancer Research Pan, Guohua; University Health Network, Campbell Family Institute for Breast Cancer Research Pauls, Henry; The Campbell Family Institute for Breast Cancer Research,



1
2
3
4
5
6
7
8
9
10
11 The Discovery of Polo-like Kinase 4 Inhibitors: Design
12 and Optimization of Spiro[cyclopropane-1,3'[3H]indol]-
13
14
15
16
17
18
19
20
21 2'(1'H)-ones as Orally Bioavailable Antitumor Agents
22
23
24

25 *Peter B. Sampson,*† Yong Liu,† Narendra Kumar Patel,† Miklos Feher,† Bryan Forrest,† Sze-Wan Li,†*
26
27 *Louise Edwards,† Radoslaw Laufer,† Yunhui Lang,† Fuqiang Ban,† Donald E. Awrey,† Guodong Mao,†*
28
29 *Olga Plotnikova,† Genie Leung,† Richard Hodgson,† Jacqueline Mason,† Xin Wei,† Reza Kiarash,† Erin*
30
31 *Green,† Wei Qiu,‡ Nickolay Y. Chirgadze,‡ Tak W. Mak,† Guohua Pan,† Henry W. Pauls†*
32
33
34
35
36
37

38 †Campbell Family Institute for Breast Cancer Research, TMDT East Tower, MaRS Centre, 101 College
39 Street, Toronto, Ontario, MG5 1L7, Canada

40 ‡Department of Pharmacology and Toxicology, University of Toronto, Toronto, Ontario M5S 1A8,
41 Canada
42
43
44

45
46 **RECEIVED DATE**
47

48
49 RUNNING TITLE: The Discovery of Novel PLK4 Inhibitors as Anticancer Agents.
50
51

52
53 ABSTRACT: Polo-like kinase 4 (PLK4), a unique member of the polo-like kinase family of serine-
54
55 threonine kinases, is a master regulator of centriole duplication that is important for maintaining genome
56
57 integrity. Overexpression of PLK4 is found in several human cancers, and is linked with a
58
59
60

1 predisposition to tumorigenesis. Previous efforts to identify potent and efficacious PLK4 inhibitors
2 resulted in the discovery of (*E*)-3-((1*H*-indazol-6-yl)methylene)indolin-2-ones which are superseded by
3 the bioisosteric 2-(1*H*-indazol-6-yl)spiro[cyclopropane-1,3'-indolin]-2'-ones reported herein.
4
5 Optimization of this new cyclopropane-linked series was based on a computational model of a PLK4 X-
6 ray structure and SAR attained from the analogous alkene-linked series. The racemic (1*R,S*,2*S,R*)
7 cyclopropane-linked compounds showed PLK4 affinity and antiproliferative activity comparable to their
8 alkene-linked congeners with improved physicochemical, ADME and pharmacokinetic properties.
9
10 Positive xenograft results from the MDA-MB-468 human breast cancer xenograft model for compound
11 **18** support the investigation of PLK4 inhibitors as anticancer therapeutics. An X-ray co-structure
12 obtained from the racemate **18** revealed preferential binding of the 1*R*,2*S* enantiomer to the PLK4 kinase
13 domain.
14
15
16
17
18
19
20
21
22
23
24
25
26

27 KEYWORDS: Polo-like Kinase 4; PLK4 inhibitors; antimetotic agents; X-ray structure; breast cancer;
28 spiro[cyclopropane-1,3'[3*H*]indol]-2'(1'*H*)-ones; MDA-MB-468 xenograft.
29
30
31
32

33 BRIEFS: Structure guided bioisosteric replacement, resulting in nanomolar PLK4 inhibitors displaying
34 potent antiproliferative activity, PLK4 co-complex X-ray structure and the results of a xenograft study
35 are described.
36
37
38
39
40

41 INTRODUCTION:

42
43

44 Blocking cell division through the inhibition of mitosis is one of the most successful clinical strategies
45 for the treatment of cancer.¹ Antimitotic drugs, such as the vinca alkaloids and taxanes, have
46 demonstrated therapeutic efficacy.² The ubiquitous role of tubulin during mitosis in both cancer and
47 normal cells, however, limits the clinical use of these antimitotics as a result of significant toxicities in
48 normal cells.² A number of mitotic kinases have been identified as having unique and essential roles in
49 cell division, and some of these are the focus of chemotherapeutic drug discovery.¹ The selectivity and
50 distinct ways in which these new targeted kinase inhibitors interfere with mitosis provide the potential
51
52
53
54
55
56
57
58
59
60

1 to not only overcome certain limitations of current antimetabolic therapeutics, but to expand the area of
2 clinical efficacy established by those drugs. The Aurora kinases, AURKA and AURKB, are established
3 druggable targets,^{1,3} with several inhibitors⁴, such as Alisertib⁵ (**1**) currently undergoing clinical
4 evaluation as anticancer agents. Another class of mitotic kinases that have gained attention as
5 therapeutic targets are the Polo-like kinases.⁶ The human polo-like kinase (PLK) family consists of five
6 serine-threonine kinases, PLK1, PLK2 (Snk), PLK3 (Fnk, Prk), PLK4 (Sak) and PLK5, and are
7 characterized by the presence of a highly conserved N-terminal catalytic domain and one or two C-
8 terminal polo-box domains.^{7,8,9} Of the five, PLK1 has been the most extensively studied and there are
9 several PLK1 inhibitors currently in Phase 1 and Phase 2 clinical trials.^{10,11}

10
11
12
13
14
15
16
17
18
19
20
21
22
23
24
25
26
27
28
29
30
31
32
33
34
35
36
37
38
39
40
41
42
43
44
45
46
47
48
49
50
51
52
53
54
55
56
57
58
59
60
PLK4 is the most structurally diverse of the PLKs, sharing little homology with the rest of the family,
possessing only one polo-box domain instead of two.^{12,13} PLK4 is a low abundance kinase present only
in proliferating tissues, and is a conserved upstream regulator of centriole duplication. PLK4 is
aberrantly expressed in breast cancer, and, in particular, the triple-negative/basal-like (TNBC) subclass,
as well as other tumor types. Upregulation of PLK4 causes centriole overduplication, and this can result
in centrosome amplification.^{14,15} Human cancers frequently contain extra centrosomes, and they are
proposed to play a causative role in genome instability and tumor development. Conversely, depletion
of PLK4 by RNA interference (RNAi) prevents centriole duplication,¹³ resulting in mitotic defects¹⁴ and
cell death. These observations were corroborated by our internal RNAi results;^{16,17} PLK4 knockdown
caused breast cancer cell death while normal cells were unaffected. In addition, PLK4 depletion was
shown to cause the suppression of breast cancer tumor growth in mice xenograft experiments. We
rationalized that small-molecule inhibition of PLK4 would potentially be beneficial therapeutically, and
recently we have reported our PLK4-directed drug discovery efforts.^{18,19}

A number of known kinase inhibitors, such as the Aurora kinase inhibitor VX-680²⁰ (**2**), and the
antiangiogenic Axitinib²¹ (**3**) are also low nM inhibitors of PLK4.²² We developed our first generation
PLK4 inhibitors from a screening exercise that yielded simple compounds with micromolar PLK4

1 activity. Subsequent iterations of structure based design, synthesis and in vitro screening yielded
2 substituted indazolyl-indolinone compounds such as **4**, **5** and **6**.¹⁹ As a class, these inhibitors displayed
3 excellent PLK4 potency, antiproliferative activity and robust tumor growth inhibition upon IP dosing.
4
5 Unfortunately, this series displayed poor pharmacokinetic properties, in particular, low oral exposure.
6
7 An additional drawback was the configurational lability inherent in these alkene-linked inhibitors. The
8 indazolylmethyleneindolinone compounds, while preferentially isolated as the E-isomer, have the
9 potential to isomerize in vivo, yielding indeterminate mixtures of *E/Z* isomers. We envisioned that
10 configurational l stability and physicochemical properties would be improved through bioisosteric
11 replacement of the double bond with a cyclopropane ring. Cyclopropanes are present in many natural
12 products and pharmaceuticals^{23,24} and have been used in drug discovery programs to prepare
13 conformationally restricted analogues of peptidomimetics²⁵ and SSRIs.²⁶ Moreover, spirocyclopropyl-
14 oxindoles have been investigated as reverse transcriptase inhibitors²⁷ and reported as kinase inhibitors.²⁸
15
16
17
18
19
20
21
22
23
24
25
26
27
28

29 Herein we describe the synthesis of 2-(1H-indazol-6-yl)spiro[cyclopropane-1,3'-indolin]-2'-ones and
30 optimization of this series as novel PLK-4 inhibitors.
31
32

33 RESULTS and DISCUSSION:

34
35 **Chemical Synthesis.** Treatment of indazol-6-ylmethyleneindolin-2-one (**7**) with
36 trimethylsulfoxonium iodide under modified Corey-Chaykovsky^{29,30} conditions, gave the racemic
37 cyclopropyl analogues in a 14:1 mixture of trans (**8**) and cis (**9**) diastereomers, as shown in Scheme 1,
38 which were separated by silica gel chromatography. The trans relative stereochemistry was defined
39 based on the work by Moldvai and coworkers as described for a series of pyridyl
40 spirocyclopropylindolones.³¹ Irradiation of the 2-H cyclopropane proton resonance only showed a NOE
41 enhancement to one of the 3-H cyclopropane protons of **8**. However, 2-H cyclopropane proton
42 resonance irradiation of compound **9** gives an NOE enhancement of the signal assigned to the 4'-H of
43 the indolone ring. Moreover, the 4'-H proton is shifted upfield in the trans conformation compared to
44
45
46
47
48
49
50
51
52
53
54
55
56
57
58
59
60

1 the cis by 1.2 ppm as a result of anisotropic shielding by the indazole ring. Thus, trans diastereomers
2 can readily be distinguished from the cis diastereomers by ¹H NMR.
3

4
5 Compounds carrying the vinyl-aryl substituent were prepared by various methods, as outlined in
6 Scheme 2 and Scheme 3. Cyclopropanation of SEM-protected indolinone **10** under Corey-Chaykovsky
7 conditions gave **11**. Cyclopropane analogues of indolinones **4** and **5** were prepared via installation of
8 the vinyl-aryl substituent under conventional Heck reaction conditions, followed by removal of the SEM
9 group by stepwise treatment with boron trifluoride etherate and 2 M HCl to give **12** and **13**.
10 Alternatively, indolinones such as **6**, **14** and **15** could be treated under Corey-Chaykovsky conditions to
11 give the cyclopropyl analogues **16**, **17** and **18** directly.
12
13
14
15
16
17
18
19
20

21 In order to prepare analogues via a more convergent route and avoid the use of protecting groups,
22 three additional synthetic paths were developed in which the cyclopropyl modification was introduced
23 at an earlier stage, and the vinyl-aryl group was installed at either the penultimate or final stage.
24 Cyclopropyl iodides (**20a-g**) were prepared under standard conditions from indolinones (**19a-g**).¹⁹ In
25 general, Heck coupling to introduce the vinyl-aryl group to cyclopropyl iodides **20a-g** either failed or
26 generated the desired compound in low yield. However, switching to Suzuki-Miyaura conditions with
27 vinylboronate esters (prepared either via rhodium catalyzed hydroboration of the corresponding terminal
28 alkyne³² or vinyl boronate Heck coupling with the appropriate aryl bromide³³) gave the desired
29 inhibitors **26-37** and **39** directly from iodides **20a-g** in better yields.
30
31
32
33
34
35
36
37
38
39
40
41
42

43 Secondly, the desired analogues were generated by treatment of **20a** under Suzuki Miyaura conditions
44 with commercially available vinyl boronate ester to give the vinylindazole **21**. The vinyl analogue, **21**
45 was then arylated under Heck conditions with the appropriate aryl bromide to give compounds **24**, **25**
46 and **38** directly in good yield. The main drawback of this route was the formation of up to 6% of a
47 branched byproduct, in which the aryl group couples to the C-1 position of the olefin.
48
49
50
51
52
53
54

55 Concurrently to the above two synthetic pathways, a reductive amination approach, was developed.
56 Compound **23** was prepared in two steps from aldehyde **22** in high selectivity as the *E*-isomer.
57
58
59
60

1 Inhibitors **40** and **41** were then prepared via reductive amination of **23** with pyrrolidine and piperidine,
2
3 respectively.

4
5 **Lead Optimization.** The rationale for morphing the (indazo-6-yl)methylene-indolin-2-ones to the
6
7 structurally analogous (indazol-6-yl)-3-spirocyclopropyl-oxindole series was to lock the molecule into a
8
9 stable configuration. Our stability studies, empirical evidence and computational models were
10
11 consistent with the *E* isomer of the (indazo-6-yl)methylene-indolin-2-ones being responsible for the
12
13 observed in vitro activity.¹⁹ However, it was not possible to unequivocally assign the biological
14
15 responses observed to this species alone. Prior to synthesis, the modification was checked
16
17 computationally to predict whether compound activity would be retained upon replacing the *E*-alkene **7**
18
19 with the trans-cyclopropane **8** (Figure 3). PLK4 docking, performed using a computational model based
20
21 on the 3COK X-ray structure,¹⁹ predicted retention of activity for this bioisosteric replacement. This was
22
23 true for molecules with or without the vinyl-aryl substitution on the indazole. It can be seen that the *E*-
24
25 form of **7** and the 1*R*,2*S* stereoisomer of **8** have nearly identical topology and similar binding poses.
26
27 Moreover their interactions with the active site and their docking scores are also similar. However, the
28
29 1*S*,2*R* enantiomer of **8** exhibits a poorer fit into the site and its docking score is about ½ log unit lower.
30
31 In absence of a facile method for enantiomeric resolution, we continued with racemic compounds for
32
33 the purposes of compound optimization.
34
35

36
37
38 Although there is a possibility of *E/Z* equilibration of the (indazol-6-yl)methylene-indolin-2-ones in
39
40 solution, we were pleased to observe that the major product from the Corey-Chaykovsky
41
42 cyclopropanation was the trans diastereomer (**8**). The minor cis diastereomer (**9**) was easily separated
43
44 by column chromatography. We were equally pleased to see that the trans-cyclopropane analogue **8**
45
46 was active against PLK4 and performed favorably with respect to the *E*-alkene congener **7** in terms of
47
48 selectivity towards Flt3 and KDR. In contrast, the cis-cyclopropane diastereomer **9**, topologically
49
50 similar to the *Z*-alkene, did not inhibit PLK4 in this assay (Table 1).
51
52
53
54
55

56
57 Furthermore, we found the cyclopropyl modification imparts improved aqueous solubility for **8** vs **7**
58
59 (8.0 µg/mL vs 0.7 µg/mL at pH 7.4). This improvement is attributed to the nature of the cyclopropane
60

1 ring, being orthogonal to the plane of the indolinone; it serves to counter crystal packing forces. The
2 cyclopropane disrupts the through-conjugation of the alkene linked system and results in a difference in
3 color between the alkene linked **7** (yellow-orange) to the cyclopropane **8** (off white). Compound **8** also
4 demonstrated desirable ADME properties, which included an improved profile for five CYP450
5 isoforms (Table 1), lower plasma protein binding (83% vs >99.9%) and better microsomal stability
6 (Table 2). Most significantly, compound **8** achieves up to 100-fold higher level of exposure in mouse
7 plasma upon IP dosing at 50 mg/kg.
8
9

10 From the preliminary PLK4 IC₅₀ values and our binding hypothesis, we reasoned that the SAR
11 observed for the (indazol-6-yl)methylene-indolin-2-ones series¹⁹ was likely transferable to the new
12 (indazol-6-yl)-3-spirocyclopropyl-oxindole scaffold. Accordingly, syntheses of cyclopropane inhibitors
13 which carry the 3-aryl-vinyl substitution on the indazole moiety, analogous to some promising leads
14 from the alkene series (Figure 2), were initiated. With the substituted analogues, there was no
15 discernible difference in the PLK4 IC₅₀ values (Table 1) or potency in the cell-proliferation assays
16 (MCF-7 and MDA-MB-468 cell lines) for cyclopropyl compounds **12**, **13** and **16** compared to alkene
17 compounds **4**, **5** and **6**, respectively (Table 2). In addition, the trend toward better aqueous solubility,
18 microsomal stability, lower plasma protein binding and KDR selectivity, held. Moreover, the selectivity
19 towards other members of the PLK family, observed in the alkene linked compounds, was recapitulated
20 in the spirocyclopropane modification (Table 3). Unfortunately, the improvement in Flt3 selectivity
21 observed for **8** (Tables 1 and 5) was not imparted to analogues carrying the vinyl aryl side chain. We
22 also observed that the 4-pyridinylvinyl analogues **4** and **12** both exhibit very strong inhibition of CYP
23 2C9 and 2C19. It appears that the 4-pyridyl function is driving this interaction, independent of the core
24 structure. Nonetheless, compounds **13** and **16** showed weak CYP450 inhibition for all five isoforms
25 tested (Table 1).
26
27
28
29
30
31
32
33
34
35
36
37
38
39
40
41
42
43
44
45
46
47
48
49
50
51
52
53

54 We were particularly gratified to see that the higher mouse plasma levels seen for the core molecule
55 carried over for elaborated analogs **12**, **13** and **16**. For example, although alkene **4** had undetectable
56 plasma levels at 50 mg/kg IP, a dramatic improvement in exposure was seen for the analogous
57
58
59
60

1 cyclopropane analogue **12** (Table 2). Going forward, efforts were focused on improving kinase
2 selectivity (e.g. Flt3), maintaining the desirable profiles seen in the first iteration of cyclopropane
3 inhibitors and to test whether this profile translated into good oral exposure.
4
5

6
7 Analogues of **12**, in which changing the position of the nitrogen in the ring, or framing the nitrogen
8 with methyl groups, such as in **17**, **24** and **25** had little effect on PLK4 activity. A moderate reduction
9 in CYP 2C9 inhibition for **24** ($IC_{50} = 400$ nM), along with a moderate improvement in cell-based
10 activity, relative to the marketed anticancer agent **3**, was observed. Modeling of **12** in the modified
11 PLK4 X-ray crystal structure (PDB code 3COK, *vide infra*) revealed that the vinyl group resided in a
12 hydrophobic groove encompassed by Leu18, and the nitrogen on the pyridine ring was pointing toward
13 the solvent interface in the same fashion observed for the alkene series.¹⁹ It was envisioned that
14 following the SAR gleaned from the alkene-linked series, the addition of solubilizing functionalities on
15 pyridyl ring would not be detrimental to PLK4 activity. Indeed, as can be seen from examples **26** and
16
17
18
19
20
21
22
23
24
25
26
27
28
29
30
31
32
33
34
35
36
37
38
39
40
41
42
43
44
45
46
47
48
49
50
51
52
53
54
55
56
57
58
59
60

Substituted styryls that carried a solvent exposed solubilizing group, were modeled and were
predicted to retain PLK4 activity compared to the 4-pyridinylvinyl analogues. As can be seen in Table
4, the nature of the solubilizing group (dimethylamine, piperidine, piperazine or morpholine) was
indiscriminant for PLK4 inhibition in general, although compounds **30** and **31** have measured PLK4
inhibition in the sub nanomolar range. However, these sub-nanomolar values should be viewed as
apparent values as they approach the nominal concentration of enzyme in the assay (PLK4
concentration = 0.4 nM).

The analogues were tested against a panel of four human breast cancer-derived cell lines (Table 4) and
compared to the structurally related compound **3**. The pyridyl compounds **12**, **16** and **24** show good
potency in the cell-based assay for MCF-7, MDA-MB-468 and MDA-MB-231 cells, although the
values for SKBr-3 remain comparable to **3**. However, potency toward the MCF-7 and MDA-MB-468
cell lines was dramatically enhanced when the tertiary amino group is added, as shown with compounds

1
2
3
4
5
6
7
8
9
10
11
12
13
14
15
16
17
18
19
20
21
22
23
24
25
26
27
28
29
30
31
32
33
34
35
36
37
38
39
40
41
42
43
44
45
46
47
48
49
50
51
52
53
54
55
56
57
58
59
60

26 and **27**. The enhanced sensitivity, relative to **3**, of these two cell lines was also observed for styryl analogues **13**, **18** and **28-41**. Overall, the responsiveness for the SKBr-3 cell line remained comparable to **3** for all the cyclopropane compounds tested.

A subset of compounds was examined for selectivity against KDR, AURKB and Flt3, compared to indolinone **4** (Table 5). The pyridyl analogues **12** and **25** showed high selectivity against KDR, but no selectivity against AURKB and Flt3, compared to **4**. Strongly basic amines, such as dimethylamino **13** and piperidine **41**, that are unsubstituted on the oxindole ring are again unselective with respect to AURKB and Flt3. However, substitution of the oxindole ring in the 5'-position, as shown with dimethylamino analogues **18** and **28**, gives high selectivity for KDR and a moderate 10 fold selectivity toward AURKB and Flt3. When a less basic solubilizing group such as morpholine is used as in **33**, **34** and **37**, a 30-50 fold PLK4/Flt3 selectivity and excellent KDR selectivity was observed. Interestingly, when a dibasic piperazine group is introduced as in **38**, 75-fold PLK4/AURKB selectivity and 50-fold PLK4/Flt3 selectivity, was attained.

The pharmacokinetic profile for select PLK4 inhibitors is shown in Table 6. Analogues such as **12**, **17** and **27**, show low oral exposure and strong CYP inhibition for the 2C9 and 2C19 isoforms. CYP inhibition was improved slightly for styryl analogues **13**, **18** and **38**, however this was not accompanied by an increase in oral exposure, likely due to the strongly basic pendent solubilizing groups. A significant improvement in C_{max} and AUC was observed for compounds **33**, **34** and **35**, which carry the less basic morpholino substituent. Compound **34** exhibited a high C_{max} of 1700 ng/mL and AUC of 4900 nghr/mL, as well as a respectable CYP inhibition profile, with IC₅₀ values greater than one micromolar for CYP 1A2, 2C9, 2C19, 2D6 and 3A4.

In vivo Efficacy. To investigate the efficacy of (indazol-6-yl)-3-spirocyclopropyl-oxindoles in vivo, compounds **13** and **18** were administered to mice bearing MDA-MB-468 breast cancer tumors in a xenograft study. Animals were dosed orally (PEG400/H₂O) at 25 mg/kg QD for 21 days. Antitumor activity was observed in vivo for each case, as shown in Figure 4. Tumor inhibition of 76% for **18** and

up to 84% for **13** was achieved, with no significant decrease in body weight by the end of the study. These results compare favorably with **2**, a known antiproliferative agent, which showed 73% inhibition (day 21) in the same xenograft model dosed IP at 50 mg/kg QD.

PLK4 X-ray Structure. Figure 5 displays the binding site, seen in the PLK4 X-ray structure co-crystallized with **18**. A hydrogen bonding network in the hinge region is shown between the indazole and the backbone carbonyl and NH of Glu90 and Cys92, respectively. Two other hydrogen bonds are observed between the oxindole and the sidechains of Lys41 and Gln160. As well, there is hydrophobic contact between the enzyme and the ligand, especially surrounding the indazole (Leu18, Ala39, Val26, Leu73 and Leu143) and encompassing the vinyl-phenyl group side chain (e.g. Leu18). The oxindole group, including the methoxy substituent, is fully embedded in a pocket surrounded by protein backbone from the top and the sides. One of the main focuses of the lead optimization effort was the placement of solubilizing functionalities in the inhibitor which could reside in a hydrophilic region when bound to PLK4. Our modified 3COK PLK4 model predicted that a viable site for inclusion of a solubilizing group was the aryl ring of the pendent vinyl-aryl group. As observed in the X-ray co-structure, the solubilizing dimethylamino functionality of **18** resides at the solvent interface.

Although the PLK4 enzyme was soaked with the racemate of **18**, only density for the *1R,2S* enantiomer is observed in the co-structure. The *1S,2R* enantiomer does not fit with the experimental electron density. This result is supported by modeling, which predicted a two log unit binding preference for the *1R,2S* enantiomer compared to the *1S,2R* enantiomer.

It is important to note that this X-ray structure and the 3COK structure enable significantly different ligand interactions. The 3COK structure is in a DFG-in conformation: the backbone of the activation loop (T-loop) runs relatively close to the plane of the fused ring system and then branches off, away from the ligand. In contrast, the co-structure of **18** is in a DFG-out conformation and the activation loop runs close to the indolinone nitrogen. In turn, the G-loop moves away in the co-structure to enable the activation loop to close down on the ligand. As a result, the 3COK site is substantially open to the

1 solvent from the distal side of the indolinone, while in our co-structure this area is essentially shielded
2
3 from the solvent, enabling further interactions with the ligand.
4
5

6 7 SUMMARY: 8

9
10 In this investigation, (indazol-6-yl)-3-spirocyclopropyl-indolin-2-ones were prepared as
11 configurationally stable congeners of the previously described (indazo-6-lyl)methylene-indolin-2-ones.
12
13 The bioisosteric replacement of the alkene linker with a cyclopropane ring serves to disrupt planarity
14 and results in potent PLK4 inhibitors with improved physicochemical properties. The (indazol-6-yl)-3-
15 spirocyclopropyl-indolin-2-one core also displays superior ADME properties, such as reduced CYP
16 inhibition and plasma protein binding and an enhanced pharmacokinetic profile in mice.
17
18
19
20
21
22
23

24 The first set of molecules, elaborated at the 3 position of the indazole moiety with a pyridinyl vinylic
25 attachment, showed high affinity for PLK4. However, these compounds exhibited significant CYP450
26 inhibition, in particular for the 2C9 isoform. Further SAR exploration revealed that there was no
27 significant difference in PLK4 inhibitory activity between pyridinylvinyl and styryl analogues.
28
29 Nonetheless, this change did serve to decrease CYP inhibition for the more sensitive isoforms into the
30 single digit micromolar range. As a group, the dialkylaminomethyl styryl analogues were potent PLK4
31 inhibitors, more soluble (especially at low pH) and effective inhibitors of breast cancer cell growth. In
32 addition, compounds **13** and **18** potently inhibited tumor growth in an MDA-MB-468 xenograft model.
33
34 Compound **18** exhibited 84 % tumor growth inhibition after 21 days, which compared favourably with
35 **2**, a well-known antimitotic agent. Pharmacokinetic properties of the inhibitors were generally
36 improved when morpholine was employed as the solubilizing group, with compounds **33**, **34** and **35**
37 showing high exposure in plasma upon oral administration in mice.
38
39
40
41
42
43
44
45
46
47
48
49
50
51

52 Although all compounds tested in this study were cyclopropyl racemates, we now have strong
53 evidence for the preferential affinity of the 1*R*,2*S* enantiomer over the 1*S*,2*R* enantiomer. Refinement of
54 the PLK4/compound **18** complex indicated density consistent with the presence of the 1*R*,2*S* enantiomer
55 in the active site. The subsequent article describes the development of a stereoselective synthesis of the
56
57
58
59
60

(indazol-6-yl)-3-spirocyclopropyl-indolin-2-ones and further optimization of the orally bioavailable morpholine analogues towards the identification of a development candidate for anticancer therapy.

EXPERIMENTAL SECTION:

Biochemical Assays. Active PLK4, as an amino terminal GST fusion of residues 1-391 of human PLK4, was purified from an *E. coli* expression system. The protein was purified from clarified cell extracts after induction at 15 °C overnight using glutathione sepharose, gel permeation chromatography, and ion exchange chromatography (Resource Q). The resulting protein was dephosphorylated with lambda phosphatase (NEB cat. no. P0753) and resolved using glutathione sepharose. The dephosphorylated GST-PLK4 was stored in aliquots at -80°C until use.

PLK4 activity was measured using an indirect ELISA detection system. Dephosphorylated GST-PLK4 (4 nM) was incubated in the presence of 15 μM ATP (Sigma cat. no. A7699), 50 mM HEPES-Na²⁺ pH 7.4, 10 mM MgCl₂, 0.01% Brij 35 (Sigma cat. no. 03-3170), in a 96-well microtitre plate pre-coated with MBP (Millipore cat# 30-011). After 30 min, the plate was washed five times with wash buffer (50 mM TRIS-Cl pH 7.4 and 0.2% Tween 20), and incubated for 30 min with a 1:3000 dilution of primary antibody (Cell Signaling cat. no. 9381). The plate was then washed 5 times with wash buffer, incubated for 30 min in the presence of secondary antibody coupled to horse radish peroxidase (BioRad cat. no. 1721019, 1:3000 concentration), washed an additional 5 times with Wash Buffer, and incubated in the presence of TMB substrate (Sigma cat. no. T0440). The colorimetric reaction was quenched after 5 min, by the addition of stop solution (0.5 N H₂SO₄), and quantified by detection at 450 nm with either a monochromatic or filter based plate reader (Molecular Devices M5 or Beckman DTX880, respectively).

Inhibition of AurB, FLT-3, KDR PLK1, PLK2 and PLK3 were determined using FRET based homogenous assays from Invitrogen. The assays were performed according to the manufacturer's

1 specifications with ATP concentrations of 25, 60, 80, 128, 940, and 156 μM , for PLK1, PLK2, PLK3,
2 AurB, FLT3, and KDR respectively.
3
4

5 Compound inhibition was determined at either a fixed concentration (10 μM) or at a variable inhibitor
6 concentration (typically 50 μM to 0.1 μM and 0.1 to 0.0002 μM in a 10 point dose response titration).
7
8 Compounds were preincubated in the presence of enzyme for 15 min prior to addition of ATP. The
9 remaining activity was quantified using the above described activity assay. The percent inhibition of a
10 compound was determined using the following formula: % inhibition = $100 \times (1 - (\text{experimental value} -$
11 background value)/(high activity control - background value)). The IC_{50} value was determined using a
12 non-linear 4 point logistic curve fit (XLfit4, IDBS) with the formula; $(A + (B / (1 + ((x/C)^D))))$, where A =
13 background value, B = range, C = inflection point, D = curve fit parameter.
14
15
16
17
18
19
20
21
22
23
24

25 Fluorogenic CYP inhibition studies were conducted at 37 $^{\circ}\text{C}$ in 96-well, round-bottom, white
26 polystyrene plates. Supersome mixtures containing CYP protein, insect control supersomes, substrate,
27 and potassium phosphate buffer (pH 7.4) were prepared with the following final concentrations: CYP
28 3A4, 4 nM 3A4+OR+b5 supersomes + 40 μM BFC in 160 mM buffer; CYP 3A4, 0.8 nM 3A4+OR+b5
29 supersomes + 0.8 μM DBF in 160 mM buffer; CYP 2D6, 6 nM 2D6+OR supersomes + 1.2 μM AMMC
30 in 40 mM buffer; CYP 2C9, 4 nM CYP 2C9+OR+ b5 + 8 μM MFC in 40 mM buffer; CYP 2C19, 4 nM
31 CYP 2C19+OR+ b5 + 20 μM CEC in 40 mM buffer; and CYP 1A2, 2 nM CYP 1A2+OR + 4 μM CEC
32 in 40 mM buffer. Reaction times were verified to be within the limits of kinetics linearity (not shown).
33 All probe substrate concentrations selected for these determinations were approximately equal to the
34 K_m . The final cofactor concentrations were 1.3 mM NADP, 3.3 mM glucose-6-phosphate and 0.4 U/mL
35 G6PDH for all enzymes. The final incubation volume was 0.2 mL. The plates were prewarmed at 37 $^{\circ}\text{C}$
36 for 10 min. The solvent concentration was constant ($\leq 0.2\%$ DMSO for test articles, $\leq 2\%$ CH_3CN for
37 positive control inhibitors) for all conditions within an experiment. Incubations were initiated by the
38 addition of prewarmed enzyme/substrate mix. After the specified incubation times (10 min for CYP
39 3A4/DBF; 15 min for CYP 1A2/CEC; 30 min for CYP 2D6/AMMC, CYP 2C19/MFC and CYP
40
41
42
43
44
45
46
47
48
49
50
51
52
53
54
55
56
57
58
59
60

3A4/BFC; 45 min for CYP 2C9/MFC) reactions were quenched by the addition of 75 μ L of 80% CH₃CN/20% 0.5 M Tris, with the exception of 3A4/DBF, which was stopped by addition of 75 μ L of 2 N NaOH. Fluorescence was then measured at the following excitation/emission wavelengths: 3A4 (485/535 nm), 2D6 (390/465 nm), and 2C9 (409/535 nm).

For data analysis, the fluorescence signals within a dilution series were normalized based on the range defined by the positive and negative control inhibitors for each isoform/substrate to 0% and 100% inhibition. The percent inhibition of a compound was determined using the same formula described above for AurB, FLT-3, KDR PLK1, PLK2 and PLK3.

Microsomal Stability Assay (Microsomal $T_{1/2}$): Test compounds were incubated at 1 μ M concentration with human, dog, rat, and mouse liver microsomes at 37 °C. The 200 μ L of reaction mixture in 100 mM Tris/HCl, pH 7.5, contained 35 μ g of microsomal protein, 9.5 μ L of NADPH Regenerating System Solution A (BD Biosciences cat. no. 451220) and 2 μ L of NADPH Regenerating System Solution B (BD Biosciences cat. no. 451200). After 0, 5, 10, 20, 40, and 60 min incubation, 20 μ L aliquots were removed from each reaction and mixed with 80 μ L of ice-cold CH₃CN. Stopped reactions were applied to a filter plate, and centrifuged at 500g for 5 min. The filtrate (60 μ L) was transferred to a fresh 96 well plate containing 100 μ L water, mixed, and the plate was sealed with a preslit silicone sealing mat. LC-MS (Bruker HCT ion trap coupled to an Agilent 1100 HPLC) was used to quantify the remaining parent. Microsoft Excel was used for the calculations. Curve fitting was used to determine k (first-order rate constant) using an exponential fit. The half-life was calculated as:
Microsomal $T_{1/2} = \ln(2)/k$.

Cell Viability Assay (GI_{50}). MDA-MB-231, MDA-MB-468, MCF-7 and SKBr-3 breast cancer cells were seeded into 96-well plates at 2500, 3000, 4000, 4000 and 4000 cells per 80 μ L, respectively, 24 h before compound overlay and cultured at 37 °C and 5% CO₂. Compounds were prepared as 10 mM DMSO stocks. Each 10 mM stock was diluted with DMEM (Dulbecco's Modified Eagle's Medium) cell

1 growth medium (Invitrogen, Burlington, ON, Canada), containing 10% FBS (fetal bovine serum) such
2 that the final concentrations ranged from 50 nM to 250 μ M. Aliquots (20 μ L) from each concentration
3 were overlaid to 80 μ L of preseeded cells to achieve final concentrations of 10 nM to 50 μ M. After 5 d,
4 the cells were fixed *in situ* by gently removing the culture media and adding 50 μ L of ice cold 10%
5 TCA per well and incubated at 4 °C for 30 min. The plates were washed with water five times and
6 allowed to air dry for 5 min. SRB (Sigma, Oakville, ON, Canada) [50 μ L of 0.4% (w/v)] solution in 1%
7 (v/v) acetic acid was added to each well, followed by incubation for 30 min at rt. The plates were
8 washed four times with 1% acetic acid to remove unbound SRB and then air dried for 5 min. The SRB
9 was solubilized with 100 μ L of 10 mM Tris pH 10.5 per well, and absorbance was read at 570 nm using
10 a SpectraPlus microplate reader (Molecular Devices Corporation). The percentage of relative inhibition
11 of cell viability was calculated by comparison to cells treated with DMSO only. GI₅₀s were calculated
12 using GraphPad PRISM software (GraphPad Software, Inc., San Diego, CA, USA). Three cell lines
13 (MDA-MB-468, MCF-7 and MDA-MB-231) generally exhibit comparable sensitivity, with the
14 inflection point for the dose response beginning at about 10 nM. Cell line SKBr-3 is less sensitive,
15 resulting in typical dose response curves where the inflection point is gradual and indistinct. For this
16 cell line, the GI₅₀ is calculated as the concentration required to inhibit cell growth at 50% of the
17 maximal response.
18
19
20
21
22
23
24
25
26
27
28
29
30
31
32
33
34
35
36
37
38
39
40

41 **Mouse Plasma Levels.** Adult female SCID mice (Princess Margaret Hospital Animal Facility,
42 Toronto, ON) were used in the experiments. All animal experiments were approved by UHN IACUC.
43 Nine mice were dosed at either 25 mg/kg (free base equivalents) via oral gavage (examples **13** and **18**)
44 or intraperitoneal injection (water with final pH adjusted to pH 4 with 1 M NaOH) using a volume of
45 200 μ L (example **2**). Saphenous vein blood was collected from three mice per time point over an 8 h
46 period. The plasma samples were analyzed by LCMS/MS for presence of drug and internal standard.
47 The pharmacokinetic parameters were calculated using Microsoft Excel with pharmacokinetic add-in
48 functions.³⁴ Parameters were calculated using plasma concentration time data for composite averages.
49
50
51
52
53
54
55
56
57
58
59
60

1 **Structural Biology.** The kinase domain fragment of human PLK4 (amino acids 6-269) was sub-
2
3 cloned into the pET_SUMO vector (Invitrogen) for bacterial expression. The protein was expressed in
4
5 *E.coli* BL21 (DE3) codon plus RIL (Stratagene) cells in TB broth media in the presence of 10% Glucose
6
7 overnight at 15 °C with 0.5 mM IPTG.
8

9
10 For the purification, the bacterial pellet was lysed in the lysis buffer (LB) supplemented with 1 mM
11
12 imidazole and 1 mM PMSF (25 mM HEPES pH 7.5, 500 mM NaCl, 10% Glycerol, and 1 mM TECEP).
13
14 After lysis using an EmulsiFlex C5 homogenizer (Avestin), the lysate was clarified by centrifugation
15
16 (50,000g for 1h at 4 °C) and loaded onto a 5 mL HiTrap Chelating column (GE Health Care), charged
17
18 with Ni²⁺. The column was washed with 10 column volumes of LB supplemented with 1 mM imidazole,
19
20 followed by 10 column volumes of LB supplemented with 50 mM imidazole, and the protein was eluted
21
22 with LB supplemented with 300 mM imidazole. SUMO protease (LifeSensors) was added to fractions
23
24 containing the PLK4 KD to remove the His6-tag and the cleavage reaction was allowed to proceed
25
26 overnight at 4 °C. The cleaved PLK4 KD protein was separated from uncleaved protein, His6_SUMO
27
28 protein, and His6_SUMO protease by loading onto a 5 mL HiTrap Chelating column (GE Health Care),
29
30 charged with Ni²⁺. The cleaved PLK4 KD was eluted from the column with LB supplemented with 50
31
32 mM imidazole while uncleaved protein, His6_SUMO protein and His6_SUMO protease were retained
33
34 on the column. The protein was loaded onto a Superdex 200 column (GE Health Care) equilibrated with
35
36 LB. The protein was further purified to homogeneity by ion-exchange chromatography.
37
38
39
40
41
42

43
44 Purified PLK4 KD was crystallized in the presence of **18** using the hanging drop vapour diffusion
45
46 method at 22 °C by mixing equal volume of the protein solution and the reservoir solution. The PLK4 -
47
48 **18** binary complex (protein:compound at a molar ratio of 1:5) was crystallized in 20% PEG 4000, 0.2 M
49
50 magnesium chloride hexahydrate, and 0.1 M Tris pH 8.5. All the crystals were soaked in the mother
51
52 liquor supplemented with 15% Glycerol as cryoprotectant before freezing in liquid nitrogen.
53
54

55
56 **X-ray Data Collection and Processing.** The X-ray data set of PLK4/compound **18** complex was
57
58 collected at an in-house facility using HF-007 Rigaku rotating anode (CuK_α) equipped with Osmic
59
60

1 VariMax focusing system and MAR-345 image detector at temperature of 100K. The diffraction data
2 were reduced and scaled with the program XDS.³⁵ The summary of crystallographic data and refinement
3 statistics are reported in the supplemental data.
4
5
6
7

8 **Structure Determination and Crystallographic Refinement.** The crystals of PLK4 complex
9 belonged to I23 space group. The initial phase of PLK4 complex was determined by molecular
10 replacement using Phaser from Phenix package.³⁶ Following the initial rigid body refinement,
11 interactive cycles of model building and refinement were carried out using COOT³⁷ and phenix.refine³⁶
12 or buster-TNT.³⁸ The coordinates and topologies of the ligands from this study were generated using
13 phenix.elbow.³⁶ Ligands were introduced at the later stages of refinement after most of the protein
14 models were built. Water molecules, as well as other solvent ligands, were added based on 2mF_o-DF_c
15 map in COOT and refined with phenix.refine or buster-TNT.
16
17
18
19
20
21
22
23
24
25
26
27

28 **Computational Methods.** In much of this work, the 3COK X-ray structure was used for modeling
29 purposes. As described previously,¹⁹ this structure was modified to enable hydrogen bonding between
30 the side chain of Lys41 and the indolinone carbonyl. The protein structure was prepared using standard
31 settings with the help of the Protein Preparation Wizard in the Schrodinger suite.³⁹ All water molecules
32 were deleted because none of them were judged as structural water (i.e. part of the binding pattern).
33 Ligands were prepared and docking results were analyzed in the MOE software,⁴⁰ appropriate
34 protonation states were generated using the Wash process, all reasonable stereoisomers were obtained
35 using Corina,⁴¹ low energy conformations were generated using Conformer Import (max. 30 conformers
36 within a 1 kcal/mol window) and minimized using the MMFF94x forcefield within MOE. These
37 conformers were all docked using GlideXP and the highest scoring solution was selected, as had been
38 recommended in order to minimize sensitivity to initial conditions.^{42,43} For cyclopropane compounds,
39 note that docking conditions typically favoured the 1*R*,2*S* form, which had ½ to 2 orders of magnitude
40 better docking scores than the 1*S*,2*R* enantiomer, hence only these forms appeared for comparison in the
41 docking scores. Mostly default conditions were applied in GlideXP docking,⁴⁴ but with the ring
42
43
44
45
46
47
48
49
50
51
52
53
54
55
56
57
58
59
60

1 conformational search switched off. Docking scores were calculated without the Epik state penalties
2 and using protein hydrogen bond constraints to the hinge (at least 1 of the hydrogen bonds to Glu90 or
3 Cys92 had to be satisfied). This model was sufficiently predictive on PLK4 ligands to enable ranking
4 (the correlation coefficient (R^2) between docking score and PLK4 pIC_{50} was 0.53 with an RMSE of 0.91
5 and $n = 553$). During the course of the study, an X-ray co-structure with **18** was obtained and a
6 docking model was generated based on this new structure. This co-structure already indicated a
7 hydrogen bond between Lys41 and the ligand, so it was applied for generating a docking model without
8 further modifications. This model provided superior performance on the same ligand set (R^2 of 0.60
9 with RMSE of 0.84 with $n = 563$) and was used in the latter stages of this work.
10
11
12
13
14
15
16
17
18
19
20
21

22 **Synthesis.** General Experimental Methods. Commercially available starting materials, reagents, and
23 solvents were used as received. In general, anhydrous reactions were performed under an inert
24 atmosphere such as nitrogen or argon. Microwave reactions were performed using a Biotage Initiator
25 microwave reactor. Reaction progress was generally monitored by TLC using Merck silica gel plates
26 with visualization by UV at 254 nm, by analytical HPLC or by LCMS (Bruker Esquire 4000). Flash
27 column chromatographic purification of intermediates or final products was performed using 230-400
28 mesh silica gel 60 from EMD chemicals or on a Biotage Isolera One purification system using SNAP
29 KP-sil cartridges. Crude reactions were partially purified using Waters PoraPak Rxn CX cartridges.
30 Preparative reverse-phase HPLC purification was performed on a Varian PrepStar model SD-1 HPLC
31 system with a Varian Monochrom 10 μ C-18 reverse-phase column. Elution was performed using a
32 gradient of 10% MeOH/water to 90% MeOH/water (0.05% TFA) over a 40-min period at a flow rate of
33 40 mL/min. Fractions containing the desired material were concentrated and lyophilized to obtain the
34 final products. Compound purity by analytical HPLC (UV detection at $\lambda = 214$ and 254 nm) was
35 performed on a Varian Prostar HPLC, using a 100 x 4.6 mm Phenomenex Luna 3 μ C-18 column.
36 Elution was performed using a gradient 10% MeOH/water to 90% MeOH/water (0.05% TFA) between
37 1 and 10 min at a flow rate of 1 mL/min. Purity is reported as area percent; the purity of all final
38
39
40
41
42
43
44
45
46
47
48
49
50
51
52
53
54
55
56
57
58
59
60

1 compounds was shown by HPLC to be $\geq 95\%$. Proton NMRs were recorded on a Bruker 400 MHz
2 spectrometer, and mass spectra were obtained using a Bruker Esquire 4000 spectrometer. All reported
3 yields are not optimized.
4
5

6
7 **Preparation of 3-spirocyclopropyl-oxindoles. General Procedure A.** To a solution of
8 trimethylsulfoxonium iodide (2 eq.) in anhydrous DMF (40 mL) was added NaH (60% dispersion in oil)
9 (6 eq.) at 0 °C. The mixture was stirred for 15 min after which time the appropriate methylene-indolin-
10 2-one (1 eq.) was added. The solution was stirred overnight at rt. The reaction was quenched with sat.
11 aq. NH₄Cl solution, extracted with 4 volumes EtOAc, dried over MgSO₄ and concentrated to dryness.
12 The major trans diastereomer was isolated by either by silica gel chromatography or preparative HPLC.
13
14
15
16
17
18
19
20

21
22 **(1*R**,2*S**)-2-(1*H*-indazol-6-yl)spiro[cyclopropane-1,3'-indolin]-2'-one (8)** The title compound was
23 prepared in a manner similar to general procedure A by utilizing **7**¹⁹ (151 mg, 0.58 mmol). The major
24 diastereomer **8** was isolated by silica gel chromatography (50% EtOAc in hexanes) as a beige solid (44
25 mg, 28%). ¹H NMR (400 MHz, DMSO-*d*₆) δ 13.01 (s, 1H), 10.61 (d, *J* = 8.3 Hz, 1H), 8.01 (s, 1H),
26 7.63 (d, *J* = 8.3 Hz, 1H), 7.44 (s, 1H), 6.99 (t, *J* = 7.5 Hz, 1H), 6.92 (d, *J* = 8.0 Hz, 1H), 6.84 (d, *J* = 8.0
27 Hz, 1H), 6.51 (t, *J* = 7.0 Hz, 1H), 5.98 (d, *J* = 8.0 Hz, 1H), 3.20–3.17 (m, 1H), 2.30–2.26 (m, 1H), 2.00–
28 1.95 (m, 1H); LCMS (ESI) *m/z* calcd for [C₁₇H₁₃N₃O+ H]⁺ 276.1; found, 276.1.
29
30
31
32
33
34
35
36
37
38

39
40 **(1*R**,2*R**)-2-(1*H*-indazol-6-yl)spiro[cyclopropane-1,3'-indolin]-2'-one (9)** The minor diastereomer
41 from the reaction of Example **8** was isolated as beige solid (3.5 mg, 2%). ¹H NMR (400 MHz, DMSO-
42 *d*₆) δ 12.97 (s, 1H), 10.33 (d, *J* = 8.3 Hz, 1H), 7.99 (s, 1H), 7.59 (d, *J* = 8.2 Hz, 1H), 7.41 (s, 1H), 7.18–
43 7.12 (m, 2H), 6.99–6.94 (m, 2H), 6.86 (d, *J* = 7.8 Hz, 1H), 3.32 (t, *J* = 8.3 Hz, 1H), 2.27–2.23 (m, 1H),
44 2.18–2.15 (m, 1H); LCMS (ESI) *m/z* calcd for [C₁₇H₁₃N₃O+ H]⁺ 276.1; found, 276.1.
45
46
47
48
49
50
51

52
53 **(1*R**,2*S**)-2-(3-iodo-1-((2-(trimethylsilyl)ethoxy)methyl)-1*H*-indazol-6-yl)spiro[cyclo-propane-**
54 **1,3'-indolin]-2'-one (11)** To a solution of trimethylsulfoxonium iodide (1.89 g, 8.6 mmol) in anhydrous
55 DMF (40 mL) was added NaH (60% dispersion in oil) (1.03 g, 25.8 mmol) at 0°C. The mixture was
56 stirred for 15 min after which time **10** (2.2 g, 4.3 mmol) was added. The solution was stirred overnight
57
58
59
60

at rt. The reaction was quenched with sat. aq. NH_4Cl solution (50 mL), extracted with EtOAc (4 x 100 mL), dried over MgSO_4 and concentrated to dryness. The title compound was isolated by silica gel chromatography (2% MeOH in CH_2Cl_2) as a yellow solid (1.5 g, 66%). ^1H NMR (400 MHz, CDCl_3) δ 7.46 (s, 1H), 7.39 (d, $J = 8.3$ Hz, 1H), 7.09 (t, $J = 7.5$ Hz, 1H), 7.04 (d, $J = 8.0$ Hz, 1H), 6.92 (d, $J = 7.8$ Hz, 1H), 6.61 (t, $J = 8.0$ Hz, 1H), 5.90 (d, $J = 8.0$ Hz, 1H), 5.70 (s, 2H), 3.57–3.53 (m, 2H), 3.49–3.44 (m, 1H), 2.31–2.28 (m, 1H), 2.12–2.09 (m, 1H), 0.89–0.84 (m, 2H), -0.05 (s, 9H); LCMS (ESI) m/z calcd for $[\text{C}_{23}\text{H}_{26}\text{IN}_3\text{O}_2\text{Si} + \text{H}]^+$ 532.1; found, 532.1.

(1R*,2S*)-(E)-2-(3-(2-(pyridin-4-yl)vinyl)-1H-indazol-6-yl)spiro-[cyclo-propane-1,3'-indolin]-2'-one (12) To a solution of **11** (375 mg, 0.7 mmol), 4-vinylpyridine (110 mg, 1.05 mmol), DIPEA (0.25 mL, 1.4 mmol) and DMF (2.5 mL) was added $\text{Pd}(\text{OAc})_2$ (8 mg, 0.035 mmol) and $\text{P}(\text{o-tol})_3$ (22 mg, 0.07 mmol). The mixture was heated under microwave irradiation (130° C) for 2 h. Ethyl acetate (150 mL) was added and the solution was washed with water (2 x 20 mL) and brine (20 mL), dried over MgSO_4 and concentrated. The residue was purified by silica gel chromatography (1:1 hexanes/EtOAc to 100% EtOAc) to give SEM-protected intermediate as a beige solid (320 mg). The material was dissolved in CH_2Cl_2 (15 mL) under an atmosphere of N_2 . Boron trifluoride etherate (1 mL) was added dropwise and the reaction was stirred for 2 h. Methylene chloride was removed *in vacuo*, and a 2:1 mixture of EtOH / 2M HCl (5 mL) was added and the reaction heated to 50 °C for 2 h. The reaction was cooled with an ice-bath and neutralized with 1 M NH_4OH to pH~8. Ethanol was removed *in vacuo* and the resulting precipitate was collected which was further purified by silica gel chromatography (15% MeOH in CH_2Cl_2) to give the title compound as a yellow solid (220 mg, 81%). ^1H NMR (400 MHz, $\text{DMSO}-d_6$) δ 13.31 (s, 1H), 10.63 (s, 1H), 8.57–8.50 (m, 2H), 8.10 (d, $J = 8.1$ Hz, 1H), 7.80 (d, $J = 16.6$ Hz, 1H), 7.75–7.70 (m, 2H), 7.50–7.42 (m, 2H), 7.09–6.99 (m, 2H), 6.85 (d, $J = 7.6$ Hz, 1H), 6.53 (t, $J = 7.5$ Hz, 1H), 6.01 (d, $J = 7.8$ Hz, 1H) 3.23–3.19 (m, 1H), 2.35–2.31 (m, 1H), 2.02–1.98 (m, 1H); HRMS (ESI) m/z calcd for $[\text{C}_{24}\text{H}_{18}\text{N}_4\text{O} + \text{H}]^+$ 379.1559; found, 379.1559; HPLC purity: 98.8% at 214 nM.

(1R*,2S*)-(E)-2-(3-(4-((dimethylamino)methyl)styryl)-1H-indazol-6-yl)spiro[cyclopropane-1,3'-indolin]-2'-one (13) To a solution of **11** (250 mg, 0.5 mmol), N,N-dimethyl-1-(4-vinylphenyl)methanamine (125 mg, 0.78 mmol), DIPEA (0.25 mL, 1.5 mmol) and DMF (1 mL) was added Pd(OAc)₂ (5 mg, 0.025 mmol) and P(o-tol)₃ (15 mg, 0.05 mmol). The mixture was heated under microwave irradiation (130 °C) for 2 h. Ethyl acetate (20 mL) was added and the solution was washed with water (2 x 5 mL) and brine (5 mL), dried over MgSO₄ and concentrated. The residue was purified by silica gel chromatography (50% to 100% EtOAc in hexanes) to give SEM-protected intermediate as a beige solid (95 mg). The material was dissolved in CH₂Cl₂ (3 mL) under an atmosphere of N₂. Boron trifluoride etherate (0.2 mL) was added dropwise and the reaction was stirred for 2 h. Methylene chloride was removed *in vacuo*, and a 2:1 mixture of EtOH / 2M HCl (0.5 mL) was added and the reaction heated to 50 °C for 2 h. The reaction was cooled with an ice-bath and neutralized with 1 M NH₄OH to pH~8. Ethanol was removed *in vacuo* and the resulting precipitate was collected which was further purified by reverse phase HPLC to give the title compound as a yellow solid (63 mg, 23%). ¹H NMR (400 MHz, CD₃OD) δ 8.02 (d, *J* = 8.3 Hz, 1H), 7.78 (d, *J* = 8.3 Hz, 2H), 7.56–7.48 (m, 5H), 7.08–7.04 (m, 2H), 6.94 (d, *J* = 8.3 Hz, 1H), 6.59 (t, *J* = 7.8 Hz, 1H), 6.00 (d, *J* = 8.0 Hz, 1H), 4.38 (s, 2H), 3.39–3.33 (m, 1H), 2.90 (s, 6H), 2.28–2.22 (m, 1H), 2.22–2.17 (m, 1H); HRMS (ESI) *m/z* calcd for [C₂₈H₂₆N₄O + H]⁺ 435.2185; found, 435.2183; HPLC purity: 98.8% at 214 nM.

(1R*,2S*)-5'-methoxy-2-(3-((E)-2-(6-(4-methylpiperazin-1-yl)pyridin-3-yl)vinyl)-1H-indazol-6-yl)spiro[cyclopropane-1,3'-indolin]-2'-one (16) The title compound was prepared according to the general procedure A using compound **6**¹⁹ (155 mg, 0.28 mmol) The crude product was purified by silica gel chromatography (5–7.5% 2 M NH₃-MeOH in DCM) to yield an 85:15 mixture of the title compound and the cis-diastereomer. The major isomer was isolated by silica gel chromatography (3–5% MeOH and 2% Et₃N in CHCl₃) to yield a sticky yellow solid which was triturated with Et₂O to give the **16** as a yellow powder (57 mg, 41%). ¹H NMR (400 MHz, CD₃OD) δ 8.26 (s, 1 H), 8.00 (d, *J* = 8.4 Hz, 1 H), 7.92 (d, *J* = 9.2 Hz, 1 H), 7.45 (s, 1 H), 7.40 (d, *J* = 16.8 Hz, 1 H), 7.28 (d, *J* = 16.8 Hz, 1 H), 7.03 (d, *J*

= 7.6 Hz, 1 H), 6.87 (d, $J = 9.2$ Hz, 1 H), 6.83 (d, $J = 8.4$ Hz, 1 H), 6.61 (dd, $J = 8.4, 2.4$ Hz, 1 H), 5.58 (d, $J = 2.0$ Hz, 1 H), 3.61 (s, 4 H), 3.39–3.37 (m, 1 H), 3.26 (s, 3 H), 2.59–2.57 (m, 4 H), 2.36 (s, 3 H), 2.25–2.17 (m, 2 H); HRMS (ESI) m/z calcd for $[C_{30}H_{30}N_6O_2 + H]^+$ 507.2508; found, 507.2802; HPLC purity: 95.6% at 214 nM.

(1R*,2S*)-2-(3-((E)-2-(pyridin-3-yl)vinyl)-1H-indazol-6-yl)spiro-[cyclopropane-1,3'-indolin]-2'-one (17) To a mixture of trimethylsulfoxonium iodide (176 mg, 0.8 mmol) and 60% NaH (96 mg, 2.4 mmol) in a RBF was added DMF (5 mL). The resulting mixture was stirred for 2 min at rt then cooled to 0 °C. A solution of (*E*)-3-((3-((*E*)-2-(pyridin-3-yl)vinyl)-1H-indazol-6-yl)methylene)indolin-2-one (**14**)¹⁹ (122 mg, 0.33 mmol) in DMF (20 mL) was added via pipette. After addition, the resulting mixture was heated at 55 °C for 2 h and cooled to rt. Additional trimethylsulfoxonium iodide (176 mg, 0.8 mmol) and 60% NaH (96 mg, 2.4 mmol) were added and the resulting mixture was stirred O/N at rt and poured onto ice (80 mL). The reaction mixture was acidified with sat. aq. NH₄Cl and extracted with EtOAc (3 x 40 mL). The combined extracts were dried (Na₂SO₄) and concentrated to give a light brown liquid. This residue was purified by flash chromatography (eluent: CH₂Cl₂ to CH₂Cl₂/MeOH/TEA = 200:10:1) to give the crude title compound as a light yellow solid which was triturated with MeOH (5 mL) and suction filtered to give the title compound as a yellow solid (43 mg, 34%). ¹H NMR (400 MHz, DMSO-*d*₆) δ 13.21 (s, 1H), 10.64 (s, 1H), 8.86 (s, 1H), 8.45 (d, $J = 3.2$ Hz, 1H), 8.15 (d, $J = 8.0$ Hz, 1H), 8.09 (d, $J = 8.4$ Hz, 1H), 7.65 (d, $J = 16.8$ Hz, 1H), 7.49 (d, $J = 16.8$ Hz, 1H), 7.47 (s, 1H), 7.40 (dd, $J = 8.0$ Hz, 4.8 Hz, 1H), 7.03 (d, $J = 8.4$ Hz, 1H), 6.99 (d, $J = 7.2$ Hz, 1H), 6.86 (d, $J = 7.6$ Hz, 1H), 6.53 (t, $J = 7.4$ Hz, 1H), 6.01 (d, $J = 7.6$ Hz, 1H), 3.21 (t, $J = 8.4$ Hz, 1H), 2.32 (dd, $J = 7.6$ Hz, 4.8 Hz, 1H), 2.00 (dd, $J = 9.0$ Hz, 4.8 Hz, 1H); HRMS (ESI) m/z calcd for $[C_{24}H_{18}N_4O + H]^+$ 379.1559; found, 379.1559; HPLC purity: 99% at 254 nM.

(1R*,2S*)-(E)-2-(3-(4-((dimethylamino)methyl)styryl)-1H-indazol-6-yl)-5'-methoxyspiro [cyclopropane-1,3'-indolin]-2'-one (18) DMF (3 mL) was added to a mixture of NaH (60%, 85 mg,

2.1 mmol) and trimethylsulfoxonium iodide (132 mg, 0.6 mmol). The resulting mixture was stirred at rt for 10 min followed by the addition of (*E*)-3-((3-(4-((dimethylamino)methyl)-styryl)-1H-indazol-6-yl)methylene)-5-methoxyindolin-2-one (**15**)¹⁹ (163 mg, 0.29 mmol) as a solution in DMF (6 mL, divided for transfer and vial rinse). The reaction was not complete after stirring at rt for 24 h. The mixture was heated at 55 °C for 1 h but was still not complete. After cooling to rt, NaH (60%, 44 mg, 1.1 mmol) and trimethylsulfoxonium iodide (69.5 mg, 0.31 mmol) was added and the mixture was heated at 55 °C for 1 h prior to quenching by addition of water (25 mL) and brine (25 mL). The mixture was extracted with EtOAc (300mL) and the organic layer was washed with brine (2 x 25 mL), dried over Na₂SO₄ and concentrated *in vacuo*. The crude product was purified by silica gel chromatography (5–7.5% 2 M NH₃-MeOH in DCM), followed by prep-HPLC to yield the title compound as a yellow TFA salt (43 mg, 32%). ¹H NMR (400 MHz, CD₃OD) δ 8.02 (d, *J* = 8.5 Hz, 1H), 7.76 (d, *J* = 8.3 Hz, 2H), 7.57–7.46 (m, 5H), 7.05 (d, *J* = 8.0 Hz, 1H), 6.84 (d, *J* = 8.3 Hz, 1H), 6.61 (dd, *J* = 2.26, 8.5 Hz, 1H), 5.58 (d, *J* = 2.5 Hz, 1H), 4.33 (s, 2H), 3.37 (t, *J* = 8.4 Hz, 1H), 3.26 (s, 3H), 2.88 (s, 6H), 2.26–2.23 (m, 1H), 2.22–2.15 (m, 1H); HRMS (ESI) *m/z* calcd for [C₂₉H₂₈N₄O₂ + H]⁺ 465.2290; found, 465.2289; HPLC purity: 95.8 % at 254 nM.

(1*R,2*S**)-2-(3-iodo-1H-indazol-6-yl)spiro[cyclopropane-1,3'-indolin]-2'-one (20a)** The title compound was prepared according to the general procedure A using **19a**¹⁹ (500 mg, 1.3 mmol) to yield **20a** as a white solid (330 mg, 64%). ¹H NMR (400 MHz, DMSO-*d*₆) δ 13.47 (s, 1H), 10.62 (s, 1H), 7.47 (s, 1H), 7.30 (d, *J* = 8.0 Hz, 1H), 7.02–6.98 (m, 2H), 6.84 (d, *J* = 7.6 Hz, 1H), 6.53 (t, *J* = 7.6 Hz, 1H), 5.97 (d, *J* = 7.6 Hz, 1H), 3.18 (t, *J* = 8.4 Hz, 1H), 2.31 (dd, *J* = 7.2 Hz, 4.8 Hz, 1H), 1.98 (dd, *J* = 8.8 Hz, 4.8 Hz, 1H); LCMS (ESI) *m/z* calcd for [C₁₇H₁₂IN₃O + H]⁺ 402.0; found, 402.0 [M + 1]⁺.

(1*R,2*S**)-2-(3-iodo-1H-indazol-6-yl)-5'-methoxyspiro-[cyclopropane-1,3'-indolin]-2'-one (20b)** The title compound was prepared according to the general procedure A using **19b**¹⁹ (658 mg, 1.6 mmol) to yield **20b** as a white solid (470 mg, 69%). ¹H NMR (400 MHz, DMSO-*d*₆) δ 13.48 (s, 1H), 10.43 (s, 1H), 7.49 (s, 1H), 7.33 (d, *J* = 8.4 Hz, 1H), 7.02 (d, *J* = 8.4 Hz, 1H), 6.74 (d, *J* = 8.4 Hz, 1H), 6.57 (dd, *J*

= 8.4 Hz, 2.4 Hz, 1H), 5.62 (d, $J = 2.4$ Hz, 1H), 3.29 (s, 3H), 3.18 (t, $J = 8.2$ Hz, 1H), 2.34 (dd, $J = 7.8$ Hz, 4.6 Hz, 1H), 1.98 (dd, $J = 9.2$ Hz, 4.8 Hz, 1H); LCMS (ESI) m/z calcd for $[C_{18}H_{14}IN_3O_2 + H]^+$ 432.1; found, 432.0.

(1*R,2*S**)-5'-fluoro-2-(3-iodo-1H-indazol-6-yl)spiro[cyclopropane-1,3'-indolin]-2'-one (20c)** The title compound was prepared according to the general procedure A using **19c**¹⁹ (160 mg, 0.39 mmol) to yield **20c** as a cream solid (89 mg, 54%). ¹H NMR (400 MHz, DMSO-*d*₆) δ 13.50 (s, 1H), 10.65 (s, 1H), 7.50 (s, 1H), 7.31 (d, $J = 8.4$ Hz, 1H), 7.00 (d, $J = 8.4$ Hz, 1H), 6.85–6.81 (m, 2H), 5.81 (d, $J = 8.4$ Hz, 1H), 3.23 (t, $J = 8.4$ Hz, 1H), 2.45–2.41 (m, 1H), 2.03–2.00 (m, 1H); LCMS (ESI) m/z calcd for $[C_{17}H_{11}FIN_3O + H]^+$ 420.0; found, 420.0.

(1*R,2*S**)-5'-ethyl-2-(3-iodo-1H-indazol-6-yl)spiro[cyclopropane-1,3'-indolin]-2'-one (20d)** To a mixture of 3-iodo-1H-indazole-6-carbaldehyde (1.36 g, 5 mmol) and 5-ethylindolin-2-one (885 mg, 5.5 mmol) in MeOH (25 mL) was added piperidine (0.1 mL, 1 mmol). The resulting mixture was refluxed for 90 min, then cooled to rt. The resulting red precipitate was collected by suction filtration and dried to give the indolinone **19d**, which was used without further purification to prepare **20d**, according to the general procedure A, as a light orange solid (710 mg, 33%). ¹H NMR (400 MHz, DMSO-*d*₆) δ 13.44 (s, 1H), 10.51 (s, 1H), 7.44 (s, 1H), 7.30 (d, $J = 8.4$ Hz, 1H), 6.99 (d, $J = 8.8$ Hz, 1H), 6.80 (d, $J = 7.2$ Hz, 1H), 6.72 (d, $J = 7.6$ Hz, 1H), 5.76 (s, 1H), 3.17 (t, $J = 7.8$ Hz, 1H), 2.29 (dd, $J = 8.0$ Hz, 4.8 Hz, 1H), 2.18–2.04 (m, 2H), 1.98 (dd, $J = 8.6$ Hz, 4.8 Hz, 1H), 0.60 (t, $J = 7.4$ Hz, 3H); LCMS (ESI) m/z calcd for $[C_{19}H_{16}IN_3O + H]^+$ 430.0; found, 430.0.

(1*R,2*S**)-5'-(difluoromethoxy)-2-(3-iodo-1H-indazol-6-yl)spiro[cyclopropane-1,3'-indolin]-2'-one (20e)** The title compound was prepared in a manner similar to general procedure A by utilizing **19e** (150 mg, 0.33 mmol) to yield **20e** as a white solid (70 mg, 45%) after purification by Biotage silica column chromatography (0 to 30% acetone gradient in hexanes). ¹H NMR (400 MHz, CDCl₃) δ 9.31 (s, 1 H), 7.40–7.43 (m, 2 H), 7.00 (d, $J = 8.4$ Hz, 1H), 6.92 (d, $J = 8.4$ Hz, 1H), 6.84–6.86 (m, 1 H), 5.99 (t,

1
2
3
4
5
6
7
8
9
10
11
12
13
14
15
16
17
18
19
20
21
22
23
24
25
26
27
28
29
30
31
32
33
34
35
36
37
38
39
40
41
42
43
44
45
46
47
48
49
50
51
52
53
54
55
56
57
58
59
60
 $J = 74$ Hz, 1H), 5.69 (s, 1H), 3.50 (t, $J = 8.8$ Hz, 1 H), 2.31–2.35 (m, 1 H), 2.10–2.15 (m, 1 H); LCMS (ESI) m/z calcd for $[C_{18}H_{12}F_2IN_3O_2 + H]^+$ 468.0; found, 468.0.

(1R*,2S*)-5'-chloro-2-(3-iodo-1H-indazol-6-yl)spiro[cyclopropane-1,3'-indolin]-2'-one (20f) To a mixture of 3-iodo-1H-indazole-6-carbaldehyde (1.36 g, 5 mmol) and 5-chloroindolin-2-one (880 mg, 5.5 mmol) in MeOH (25 mL) was added piperidine (0.1 mL, 1 mmol). The resulting mixture was refluxed for 90 min, then cooled to rt. The resulting yellow precipitate was collected by suction filtration and dried to give the indolinone **19f**, which was used without further purification to prepare **20f**, according to the general procedure A, as a light beige solid (2.29 g, quantitative). 1H NMR (400 MHz, DMSO- d_6) δ 13.51 (s, 1H), 10.76 (s, 1H), 7.52 (s, 1H), 7.33 (d, $J = 8.0$ Hz, 1H), 7.04 (t, $J = 8.8$ Hz, 2H), 6.84 (d, $J = 8.4$ Hz, 1H), 6.03 (s, 1H), 3.23 (t, $J = 8.0$ Hz, 1H), 2.06–1.97 (m, 2H); LCMS (ESI) m/z calcd for $[C_{17}H_{11}ClIN_3O + H]^+$ 436.0; found, 436.2.

(1R*,2S*)-2-(3-iodo-1H-indazol-6-yl)-5'-methylspiro[cyclopropane-1,3'-indolin]-2'-one (20g) To a mixture of 3-iodo-1H-indazole-6-carbaldehyde (1.36 g, 5 mmol) and 5-methylindolin-2-one (772 mg, 5.25 mmol) in MeOH (25 mL) was added piperidine (0.1 mL, 1 mmol). The resulting mixture was refluxed for 90 min, then cooled to rt. The resulting yellow precipitate was collected by suction filtration and dried to give the indolinone **19g**, which was used without further purification to prepare **20f**, according to the general procedure A, as a yellow solid and a 6:1 mixture of diastereomers (2.06 g, 99%) which was used without further purification. 1H NMR (400 MHz, DMSO- d_6) δ 13.43 (s, 1H), 10.51 (s, 1H), 7.47 (s, 1H), 7.32 (d, $J = 8.4$ Hz, 1H), 7.02 (d, $J = 8.8$ Hz, 1H), 6.81 (d, $J = 8.4$ Hz, 1H), 6.73 (d, $J = 7.6$ Hz, 1H), 5.86 (s, 1H), 3.18 (t, $J = 8.2$ Hz, 1H), 2.30–2.20 (m 1H), 2.00–1.90 (m, 1H), 1.85 (s, 3H); LCMS (ESI) m/z calcd for $[C_{18}H_{14}IN_3O + H]^+$ 416.0; found, 416.1.

(1R*,2S*)-2-(3-vinyl-1H-indazol-6-yl)spiro[cyclopropane-1,3'-indolin]-2'-one (21) To a mixture of **20a** (802 mg, 2 mmol) and 4,4,5,5-tetramethyl-2-vinyl-1,3,2-dioxaborolane (462 mg, 3 mmol) in a 20 mL microwave vial was added PhCH₃/EtOH (8 mL/4 mL), followed by 1 M aq. Na₂CO₃ (3 mL, 3

mmol) and Pd(PPh₃)₄ (46 mg, 0.04 mmol, 2 mol%) and the resulting mixture was purged with argon and microwaved 3 h at 120 °C. After aqueous workup, the solution was extracted with EtOAc and was purified by flash chromatography (50% hexanes in EtOAc) to give the crude title compound as a light yellow foam (512 mg) which was used without further purification. ¹H NMR (400 MHz, CDCl₃) δ 7.74 (d, *J* = 8.4 Hz, 1H), 7.35 (s, 1H), 7.10–6.88 (m, 5H), 6.54 (t, *J* = 7.4 Hz, 1H), 6.06 (d, *J* = 18.0 Hz, 1H), 5.92 (d, *J* = 7.6 Hz, 1H), 5.49 (d, *J* = 7.6 Hz, 1H), 3.46 (d, *J* = 8.2 Hz, 1H), 2.30–2.18 (m, 2H); LCMS (ESI) *m/z* calcd for [C₁₉H₁₅N₃O + H]⁺ 302.1; found, 302.0.

4-((*E*)-2-(6-((1*R,2*S**)-2'-oxospiro[cyclopropane-1,3'-indoline]-2-yl)-1H-indazol-3-yl)vinyl)benzaldehyde (23)** Diethyl 4-cyanobenzylphosphonate (600 mg, 2.4 mmol) was dissolved in DMF (5 mL) at 0 °C. Potassium *tert*-butoxide (540 mg, 4.8 mmol) was added and the mixture was stirred for 5 min. 6-((1*R**,2*S**)-2'-oxospiro[cyclopropane-1,3'-indoline]-2-yl)-1H-indazole-3-carbaldehyde **22** (200 mg, 0.66 mmol) was dissolved into DMF (5 mL), added dropwise and the reaction mixture was stirred for 90 min. The reaction was neutralized with aq. HCl (0.1 N) and the resulting precipitate collected. The precipitate was dissolved in EtOAc (100 mL) and washed with H₂O (2 x 10 mL), brine (10 mL), dried over MgSO₄ and concentrated to dryness. The residue was purified by silica gel chromatography to give 4-((*E*)-2-(6-((1*R**,2*S**)-2'-oxospiro[cyclopropane-1,3'-indoline]-2-yl)-1H-indazol-3-yl)vinyl)benzonitrile as a white solid (100 mg, 38%). ¹H NMR (400 MHz, CD₃OD) δ 8.04 (d, *J* = 8.5 Hz, 1H), 7.82 (d, *J* = 8.6 Hz, 2H), 7.74 (d, *J* = 8.6 Hz, 2H), 7.66–7.53 (m, 2H), 7.48 (s, 1H), 7.08–7.04 (m, 2H), 6.94 (d, *J* = 8.3 Hz, 1H), 6.59 (t, *J* = 7.6 Hz, 1H), 5.99 (d, *J* = 7.5 Hz, 1H), 3.38–3.34 (m, 1H), 2.27–2.18 (m, 2H); LCMS (ESI) *m/z* calcd for [C₂₆H₁₈N₄O + H]⁺ 403.1; found 403.1. The nitrile (100 mg, 0.25 mmol) was then dissolved in pyridine (3 mL), acetic acid (0.8 mL) and water (1 mL). Raney Nickel (100 mg), was added, following by dropwise addition of aqueous sodium hypophosphite (180 mg, 2.1 mmol in 1 mL of water) and the reaction was stirred overnight at 60 °C. The product was extracted into EtOAc (30 mL), washed with brine (5 mL), dried over MgSO₄ and concentrated to dryness. The residue was purified by silica gel chromatography (99:1 CH₂Cl₂/MeOH)

1 to give the title compound as an orange solid (95 mg, 94%). ¹H NMR (400 MHz, CDCl₃) δ 10.03 (s,
2 1H), 8.20 (s, 1H), 7.86–7.97 (m, 2H), 7.74 (d, *J* = 8.3 Hz, 1H), 7.57 (d, *J* = 8.0 Hz, 1H), 7.41 (s, 1H),
3 7.07–7.13 (m, 2H), 6.88–7.03 (m, 2H), 6.63 (t, *J* = 7.5 Hz, 1H), 5.94 (d, *J* = 7.8 Hz, 1H), 3.40 (t, *J* = 7.1
4 Hz, 1H), 2.35–2.44 (m, 1H), 2.08–2.02 (m, 1H); LCMS (ESI) *m/z* calcd for [C₂₆H₁₉N₃O₂ + H]⁺ 406.2;
5 found, 406.2.
6
7
8
9
10

11 Heck Arylation of 3-vinylspirocyclopropaneindolinones. General Procedure B.

12 To a mixture of 2-(3-vinyl-1H-indazol-6-yl)spiro[cyclopropane-1,3'-indolin]-2'-one (1 eq.) and
13 arylbromide (1 eq.) in DMF was added DIPEA (2 eq.), followed by Pd(OAc)₂ (5 mol%) and P(*o*-tol)₃
14 (10 mol%). The resulting mixture was purged with argon, and then microwaved 2 h at 125 °C. The
15 mixture was filtered through a Waters PoraPak CX column and then purified by preparative HPLC.
16
17
18
19
20
21
22
23
24
25

26 **(1*R*,2*S*)-2-(3-((*E*)-2-(6-methylpyridin-3-yl)vinyl)-1H-indazol-6-yl)spiro[cyclopropane-1,3'-**
27 **indolin]-2'-one (24)** The title compound was prepared according to general procedure B using **21** (60
28 mg, 0.2 mmol) and 5-bromo-2-methylpyridine (34.4 mg, 0.2 mmol). Purification by preparative HPLC
29 gave **24** as a light yellow solid (25 mg, 25%) contaminated with ~6% of the branched isomer. ¹H NMR
30 (400 MHz, CD₃OD) δ 8.90 (s, 1H), 7.74 (dd, *J* = 8.4 Hz, 1.6 Hz, 1H), 8.02 (d, *J* = 8.4 Hz, 1H), 7.87 (d,
31 *J* = 8.4 Hz, 1H), 7.78 (d, *J* = 16.8 Hz, 1H), 7.55 (d, *J* = 16.8 Hz, 1H), 7.49 (s, 1H), 7.07–7.00 (m, 2H),
32 6.94 (d, *J* = 8.0 Hz, 1H), 6.55 (t, *J* = 7.6 Hz, 1H), 5.97 (d, *J* = 7.6 Hz, 1H), 3.34 (t, *J* = 8.4 Hz, 1H), 2.78
33 (s, 3H), 2.23 (dd, *J* = 7.6 Hz, 4.8 Hz, 1H), 2.18 (dd, *J* = 8.8 Hz, 4.8 Hz, 1H); HRMS (ESI) *m/z* calcd for
34 [C₂₅H₂₀N₄O + H]⁺ 393.1715; found, 393.1711; HPLC purity: 94% at 214 nM.
35
36
37
38
39
40
41
42
43
44
45
46
47
48

49 **(1*R**,2*S**)-2-(3-((*E*)-2-(2,6-dimethylpyridin-3-yl)vinyl)-1H-indazol-6-yl)spiro[cyclopropane-1,3'-**
50 **indolin]-2'-one (25)** The title compound was prepared according to general procedure B using **21** (60
51 mg, 0.2 mmol) and 3-bromo-2,6-dimethylpyridine (37 mg, 0.2 mmol). Purification by preparative
52 HPLC gave **25** as a light yellow solid (23 mg, 22%) contaminated with ~3% of the branched isomer. ¹H
53 NMR (400 MHz, CD₃OD) δ 8.73 (d, *J* = 8.0 Hz, 1H), 7.97 (d, *J* = 8.4 Hz, 1H), 7.72 (d, *J* = 8.4 Hz, 1H),
54
55
56
57
58
59
60

7.68 (d, $J = 16.4$ Hz, 1H), 7.59 (d, $J = 16.4$ Hz, 1H), 7.50 (s, 1H), 7.06 (d, $J = 8.8$ Hz, 1H), 7.05 (t, $J = 8.6$ Hz, 1H), 6.94 (d, $J = 8.0$ Hz, 1H), 6.56 (t, $J = 7.6$ Hz, 1H), 5.98 (d, $J = 7.6$ Hz, 1H), 3.35 (t, $J = 8.4$ Hz, 1H), 2.86 (s, 3H), 2.76 (s, 3H), 2.24 (dd, $J = 7.6$ Hz, 4.8 Hz, 1H), 2.18 (dd, $J = 9.0$ Hz, 5.0 Hz, 1H); HRMS (ESI) m/z calcd for $[C_{26}H_{22}N_4O + H]^+$ 407.1872; found, 407.1877; HPLC purity: 96.9% at 214 nM.

Suzuki-Miyaura cross coupling of 3-iodospirocyclopropaneindolinones. General Procedure C.

The appropriate 2-(3-iodo-1H-indazol-6-yl)spiro[cyclopropane-1,3'-indolin]-2'-one **20** (1 eq.) was dissolved into 2:1 PhCH₃/EtOH and 1 M Na₂CO₃ (2 eq.). The appropriate vinyl boronic ester (1.2 eq.) and catalyst, Pd(PPh₃)₄ (5 mol%) were added and resulting mixture was heated in a microwave for 2 h at 125 °C. After cooling to rt, the mixture was diluted with H₂O, extracted with EtOAc (x 2) and dried (MgSO₄). After removal of solvents, the residue was redissolved in MeOH and filtered through a Waters CX column and purified by preparative HPLC to give the title compound as a TFA salt.

(1R*,2S*)-(E)-2-(3-((E)-2-(6-(piperidin-1-ylmethyl)pyridin-3-yl)vinyl)-1H-indazol-6-yl)spiro[cyclopropane-1,3'-indolin]-2'-one (26) The title compound was synthesized according to the general procedure C using **20a** (50 mg, 0.12 mmol) and (*E*)-2-(piperidin-1-ylmethyl)-5-(2-(4,4,5,5-tetramethyl-1,3,2-dioxaborolan-2-yl)vinyl)pyridine (65 mg, 0.2 mmol). Purification by reverse phase preparative HPLC gave **26** as a yellow TFA salt (9 mg, 15%). ¹H NMR (400 MHz, CD₃OD) δ 8.91 (s, 1H), 8.20 (dd, $J = 8.2, 2.0$ Hz, 1H), 8.04 (d, $J = 8.0$ Hz, 1H), 7.68–7.49 (m, 4H), 7.08–7.04 (m, 2H), 6.95 (d, $J = 7.8$ Hz, 1H), 6.60–6.56 (m, 1H), 5.99 (d, $J = 7.5$ Hz, 1H), 4.45 (s, 2H) 3.39–3.10 (m, 3H), 2.27–2.18 (m, 2H), 1.95–1.60 (m, 8H); HRMS (ESI) m/z calcd for $[C_{30}H_{29}N_5O + H]^+$ 476.2450; found, 476.2448; HPLC purity: 97.8% at 214 nM.

(1R*,2S*)-5'-methoxy-2-(3-((E)-2-(6-(piperidin-1-ylmethyl)pyridin-3-yl)vinyl)-1H-indazol-6-yl)spiro[cyclopropane-1,3'-indolin]-2'-one (27) The title compound was synthesized according to the general procedure C using **20b** (51 mg, 0.12 mmol) and (*E*)-2-(piperidin-1-ylmethyl)-5-(2-(4,4,5,5-

1 tetramethyl-1,3,2-dioxaborolan-2-yl)vinyl)pyridine (65 mg, 0.2 mmol). Purification by reverse phase
2 preparative HPLC gave **27** as a yellow TFA salt (15 mg, 21%). ¹H NMR (400 MHz, CD₃OD) δ 8.90 (d,
3 *J* = 1.2 Hz, 1H), 8.19 (dd, *J* = 8.2, 1.8 Hz, 1H), 8.05 (d, *J* = 8.0 Hz, 1H), 7.67–7.51 (m, 4H), 7.07 (d, *J* =
4 8.3 Hz, 1H), 6.84 (d, *J* = 8.3 Hz, 1H), 6.62 (dd, *J* = 8.5, 2.5 Hz, 1H), 5.58 (d, *J* = 2.3 Hz, 1H), 4.45 (s,
5 2H), 3.39–3.10 (m, 3H), 3.27 (s, 3H), 2.27–2.17 (m, 2H), 1.95–1.80 (m, 5H), 1.80–1.60 (m, 3H); HRMS
6 (ESI) *m/z* calcd for [C₃₁H₃₁N₅O₂ + H]⁺ 506.2556; found, 506.2562; HPLC purity: 97.9% at 214 nM.
7
8
9
10
11
12
13

14
15 **(1*R**,2*S**)-(*E*)-5'-difluoromethoxy-2-(3-(4-((dimethylamino)methyl)styryl)-1*H*-indazol-6-**
16 **yl)spiro[cyclopropane-1,3'-indolin]-2'-one (**28**)** The title compound was synthesized according to the
17 general procedure C, by using **20e** (75 mg, 0.16 mmol) and (*E*)-*N,N*-dimethyl-1-(4-(2-(4,4,5,5-
18 tetramethyl-1,3,2-dioxaborolan-2-yl)vinyl)phenyl)methanamine (58 mg, 0.20 mmol). Purification by
19 preparative HPLC gave **28** as an off-white TFA salt (38 mg, 39%). ¹H NMR (400 MHz, CD₃OD) δ
20 8.03 (d, *J* = 8.4 Hz, 1H), 7.76 (d, *J* = 8.0 Hz, 2H), 7.55–7.48 (m, 5H), 7.03 (d, *J* = 8.4 Hz, 1H), 6.91 (d, *J* =
21 8.4 Hz, 1H), 6.84 (d, *J* = 8.4 Hz, 1H), 6.14 (t, *J* = 74.4 Hz, 1H), 5.77 (s, 1H), 4.33 (s, 2H), 3.41 (t, *J* =
22 8.4 Hz, 1H), 2.88 (s, 6H), 2.33–2.30 (m, 1H), 2.25–2.21 (m, 1H); HRMS (ESI) *m/z* calcd for
23 [C₂₉H₂₆F₂N₄O₂ + H]⁺ 501.2102; found, 501.2098; HPLC purity: >99.9% at 254 nM.
24
25
26
27
28
29
30
31
32
33
34
35
36
37

38 **(1*R**,2*S**)-(*E*)-5'-chloro-2-(3-(4-((dimethylamino)methyl)styryl)-1*H*-indazol-6-yl)spiro**
39 **[cyclopropane-1,3'-indolin]-2'-one (**29**)** The title compound was prepared according to general
40 procedure C from **20f** (44 mg, 0.1 mmol) and (*E*)-*N,N*-dimethyl-1-(4-(2-(4,4,5,5-tetramethyl-1,3,2-
41 dioxaborolan-2-yl)vinyl)phenyl)methanamine (43 mg, 0.15 mmol) to give **29** as a light yellow TFA salt
42 (29 mg, 50%). ¹H NMR (400 MHz, CD₃OD) δ 8.03 (d, *J* = 8.4 Hz, 1H), 7.75 (d, *J* = 8.0 Hz, 2H), 7.55–
43 7.47 (m, 5H), 7.06–7.01 (m, 2H), 6.90 (d, *J* = 8.4 Hz, 1H), 5.97 (s, 1H), 4.33 (s, 2H), 3.39 (t, *J* = 8.4 Hz,
44 1H), 2.88 (s, 6H), 2.29 (dd, *J* = 8.0 Hz, 5.2 Hz, 1H), 2.21 (dd, *J* = 8.8 Hz, 4.8 Hz, 1H); HRMS (ESI) *m/z*
45 calcd for [C₂₈H₂₅ClN₄O + H]⁺ 469.1795; found, 469.1791; HPLC purity: 99.6% at 214 nM.
46
47
48
49
50
51
52
53
54
55
56
57
58
59
60

(1*R,2*S**)-(*E*)-2-(3-(4-((dimethylamino)methyl)styryl)-1*H*-indazol-6-yl)-5'-methylspiro**

[cyclopropane-1,3'-indolin]-2'-one (30) The title compound was prepared according to general procedure C using **20g** (42 mg, 0.1 mmol) and (*E*)-*N,N*-dimethyl-1-(4-(2-(4,4,5,5-tetramethyl-1,3,2-dioxaborolan-2-yl)vinyl)phenyl)methanamine (43 mg, 0.15 mmol) to give **30** as a yellow TFA salt (27 mg, 48%). ¹H NMR (400 MHz, CD₃OD) δ 8.00 (d, *J* = 8.4 Hz, 1H), 7.75 (d, *J* = 8.0 Hz, 2H), 7.53 (s, 2H), 7.52 (d, *J* = 8.8 Hz, 2H), 7.46 (s, 1H), 7.03 (d, *J* = 8.4 Hz, 1H), 6.86 (d, *J* = 8.0 Hz, 1H), 6.82 (d, *J* = 7.6 Hz, 1H), 5.83 (s, 1H), 4.33 (s, 2H), 3.32 (t, *J* = 8.4 Hz, 1H), 2.88 (s, 6H), 2.22–2.13 (m, 2H), 1.88 (s, 3H); HRMS (ESI) *m/z* calcd for [C₂₉H₂₈N₄O + H]⁺ 449.2341; found, 449.2333; HPLC purity: 99.8% at 214 nM.

(1*R,2*S**)-(*E*)-2-(3-(4-((dimethylamino)methyl)styryl)-1*H*-indazol-6-yl)-5'-fluorospiro**

[cyclopropane-1,3'-indolin]-2'-one (31) The title compound was synthesized according to the general procedure C by using **20c** (75 mg, 0.178 mmol) and (*E*)-*N,N*-dimethyl-1-(4-(2-(4,4,5,5-tetramethyl-1,3,2-dioxaborolan-2-yl)vinyl)phenyl)methanamine (64 mg, 0.22 mmol). Purification by preparative HPLC gave **31** as a cream colored TFA salt (42 mg, 41%). ¹H NMR (400 MHz, CD₃OD) δ 8.04 (d, *J* = 8.4 Hz, 1H), 7.77 (d, *J* = 8.0 Hz, 2H), 7.57 (s, 2H), 7.56–7.50 (m, 3H), 7.05 (d, *J* = 8.4 Hz, 1H), 6.91–6.88 (m, 1H), 6.82–6.77 (m, 1H), 5.77 (dd, *J* = 8.8 Hz, 2.4 Hz, 1H), 4.33 (s, 2H), 3.42–3.38 (m, 1H), 2.88 (s, 6H), 2.32–2.29 (m, 1H), 2.24–2.20 (m, 1H); HRMS (ESI) *m/z* calcd for [C₂₈H₂₅FN₄O + H]⁺ 453.2091; found, 453.2089; HPLC purity: 99.9% at 254 nM.

(1*R,2*S**)-(*E*)-2-(3-(4-((dimethylamino)methyl)styryl)-1*H*-indazol-6-yl)-5'-ethylspiro**

[cyclopropane-1,3'-indolin]-2'-one (32) The title compound was synthesized according to the general procedure C by using **20d** (42.9 mg, 0.1 mmol) and (*E*)-*N,N*-dimethyl-1-(4-(2-(4,4,5,5-tetramethyl-1,3,2-dioxaborolan-2-yl)vinyl)phenyl)methanamine (29 mg, 0.1 mmol) Purification by preparative HPLC gave **32** as a white TFA salt (19 mg, 34%). ¹H NMR (400 MHz, CD₃OD) δ 8.01 (d, *J* = 8.8 Hz, 1H), 7.76 (d, *J* = 8.0 Hz, 2H), 7.54–7.50 (m, 4H), 7.44 (s, 1H), 7.04 (d, *J* = 8.4 Hz, 1H), 6.86 (d, *J* = 8.0 Hz, 1H), 6.82 (d, *J* = 8.0 Hz, 1H), 5.77 (s, 1H), 4.33 (s, 2H), 3.34 (t, *J* = 8.0 Hz, 1H), 2.88 (s, 6H), 2.25–

2.10 (m, 4H), 0.65 (t, $J = 7.6$ Hz, 3H); HRMS (ESI) m/z calcd for $[C_{30}H_{30}N_4O + H]^+$ 463.2498; found, 463.22505; HPLC purity: 99% at 254 nM.

(1*R,2*S**)-(*E*)-2-(3-(4-(morpholinomethyl)styryl)-1*H*-indazol-6-yl)spiro[cyclopropane-1,3'-indolin]-2'-one (33)** The title compound was synthesized according to the general procedure C by using **20a** (50 mg, 0.12 mmol) and (*E*)-4-(4-(2-(4,4,5,5-tetramethyl-1,3,2-dioxaborolan-2-yl)vinyl)benzyl)morpholine (65 mg, 0.2 mmol). The residue was purified by reversed phase preparatory HPLC to give **33** as a pale yellow TFA salt (30 mg, 41%). 1H NMR (400 MHz, CD_3OD) δ 8.02 (d, $J = 8.5$ Hz, 1H), 7.78 (d, $J = 8.6$ Hz, 2H), 7.75–7.48 (m, 5H), 7.08–7.05 (m, 2H), 6.94 (d, $J = 8.3$ Hz, 1H), 6.59 (t, $J = 7.6$ Hz, 1H), 5.99 (d, $J = 7.5$ Hz, 1H), 4.39 (s, 2H), 4.12–4.04 (m, 2H), 3.79–3.68 (m, 2H), 3.44–3.34 (m, 3H), 3.30–3.19 (m, 2H), 2.28–2.16 (m, 2H); HRMS (ESI) m/z calcd for $[C_{30}H_{28}N_4O_2 + H]^+$ 477.2291; found, 477.2286; HPLC purity: 96.4% at 214 nM.

(1*R,2*S**)-(*E*)-5'-methoxy-2-(3-(4-(morpholinomethyl)styryl)-1*H*-indazol-6-yl)spiro[cyclopropane-1,3'-indolin]-2'-one (34)** The title compound was synthesized according to the general procedure C, using **20b** (30 mg, 0.07 mmol) and (*E*)-4-(4-(2-(4,4,5,5-tetramethyl-1,3,2-dioxaborolan-2-yl)vinyl)benzyl)morpholine (30 mg, 0.091 mmol). Purification by column chromatography (5–6% MeOH in $CH_2Cl_2/MeOH$) gave crude material which was further purified by preparative HPLC to give **34** as a white TFA salt (18 mg, 51%); 1H NMR (400 MHz, CD_3OD) δ 8.04 (d, $J = 8.4$ Hz, 1H), 7.78 (d, $J = 8.2$ Hz, 2H), 7.57–7.50 (m, 5H), 7.07 (d, $J = 8.6$ Hz, 1H), 6.83 (d, $J = 8.5$ Hz, 1H), 6.61 (dd, $J = 8.5$ Hz, 2.2 Hz, 1H), 5.58 (d, $J = 2.2$ Hz, 1H), 4.39 (s, 2H), 4.09–4.04 (m, 2H), 3.78–3.72 (m, 2H), 3.43–3.33 (m, 3H), 3.27–3.20 (m, 5H), 2.27–2.23 (m, 1H), 2.21–2.16 (m, 1H); HRMS (ESI) m/z calcd for $[C_{31}H_{30}N_4O_3 + H]^+$ 507.2396; found, 507.2387; HPLC purity: 95.0% at 214 nM.

(1*R*,2*S*)-5'-fluoro-2-(3-((*E*)-4-(morpholinomethyl)styryl)-1*H*-indazol-6-yl)spiro[cyclopropane-1,3'-indolin]-2'-one (35) The title compound was synthesized according to the general procedure C, using **20c** (60.0 mg, 0.139 mmol) and (*E*)-4-(4-(2-(4,4,5,5-tetramethyl-1,3,2-dioxaborolan-2-

1 yl)vinyl)benzyl)morpholine (54 mg, 0.17 mmol). Purification by preparative HPLC gave **35** as a cream
2
3 TFA salt (31 mg, 37%). ¹H NMR (400 MHz, CD₃OD) δ 8.04 (d, *J* = 8.8 Hz, 1H), 7.77 (d, *J* = 7.2 Hz,
4
5 2H), 7.59–7.52 (m, 5H), 7.05 (d, *J* = 8.0 Hz, 1H), 6.91–6.88 (m, 1H), 6.79 (t, *J* = 8.0 Hz, 1H), 5.74 (d, *J*
6
7 = 8.8 Hz, 1H), 4.39 (s, 2H), 4.08–4.05 (bm, 2H), 3.76–3.70 (m, 2H), 3.42–3.35 (m, 3H), 3.26–3.23 (m,
8
9 2H), 2.30 (t, *J* = 5.6 Hz, 1H), 2.24–2.20 (m, 1H); HRMS (ESI) *m/z* calcd for [C₃₀H₂₇FN₄O₂ + H]⁺
10
11 495.2196; found 495.2193; HPLC purity: 99.9% at 254 nM.
12
13

14
15 **(1*R**,2*S**)-(*E*)-5'-methyl-2-(3-(4-(morpholinomethyl)styryl)-1H-indazol-6-yl)spiro[cyclopropane-**
16
17 **1,3'-indolin]-2'-one (36)** The title compound was prepared using the general procedure C using **20g** (83
18 mg, 0.2 mmol) and (*E*)-4-(4-(2-(4,4,5,5-tetramethyl-1,3,2-dioxaborolan-2-yl)vinyl)benzyl)morpholine
19
20 (66 mg, 0.2 mmol) to give **36** as a yellow TFA salt (27 mg, 22%). ¹H NMR (400 MHz, CD₃OD) δ 7.73
21
22 (d, *J* = 8.4 Hz, 1H), 7.53 (d, *J* = 8.0 Hz, 2H), 7.44 (d, *J* = 8.0 Hz, 2H), 7.38 (s, 1H), 7.32 (d, *J* = 16.8 Hz,
23
24 1H), 7.27 (d, *J* = 16.8 Hz, 1H), 6.82 (d, *J* = 8.4 Hz, 1H), 6.77 (d, *J* = 8.0 Hz, 1H), 6.73 (d, *J* = 8.0 Hz,
25
26 1H), 5.78 (s, 1H), 4.29 (s, 2H), 3.99 (d, *J* = 11.2 Hz, 2H), 3.75 (t, *J* = 11.6 Hz, 2H), 3.42–3.32 (m, 2H),
27
28 3.21 (t, *J* = 8.4 Hz, 1H), 3.18–3.08 (m, 2H), 2.09–2.01 (m, 2H), 1.72 (s, 3H); HRMS (ESI) *m/z* calcd for
29
30 [C₃₁H₃₀N₄O₂ + H]⁺ 491.2447; found, 491.446; HPLC purity: 99.7% at 214 nM.
31
32
33
34
35
36
37

38 **(1*R**,2*S**)-2-(3-(3,5-difluoro-4-(morpholinomethyl)styryl)-1H-indazol-6-yl)-5'-methoxyspiro**
39
40 **[cyclopropane-1,3'-indolin]-2'-one (37)** The title compound was synthesized according to the general
41
42 procedure C using **20b** (60 mg, 0.14 mmol) and (*E*)-4-(2,6-difluoro-4-(2-(4,4,5,5-tetramethyl-1,3,2-
43
44 dioxaborolan-2-yl)vinyl)benzyl)morpholine (58 mg, 0.16 mmol). Purification by preparative HPLC
45
46 gave **37** as a cream TFA salt (29 mg, 27%). ¹H NMR (400 MHz, CD₃OD) δ 8.03 (d, *J* = 8.8 Hz, 1H),
47
48 7.63 (d, *J* = 16.8 Hz, 1H), 7.52–7.49 (m, 4H), 7.06 (s, *J* = 8.4 Hz, 1H), 6.82 (d, *J* = 8.4 Hz, 1H), 6.60 (d,
49
50 *J* = 8.8 Hz, 1H), 5.57 (s, 1H), 4.51 (s, 2H), 4.10–3.72 (m, 4H), 3.47–3.42 (m, 5H), 3.26 (s, 3H), 2.26–
51
52 2.23 (m, 1H), 2.21–2.17 (m, 1H); HRMS (ESI) *m/z* calcd for [C₃₁H₂₈F₂N₄O₃ + H]⁺ 543.2208; found,
53
54 543.2201; HPLC purity: 99.8% at 254 nM.
55
56
57
58
59
60

(1*R,2*S**)-(*E*)-2-(3-(4-((4-methylpiperazin-1-yl)methyl)styryl)-1*H*-indazol-6-yl)spiro**

[cyclopropane-1,3'-indolin]-2'-one (38) The title compound was prepared according to general procedure B using **21** (60 mg, 0.2 mmol) and 1-(4-bromobenzyl)-4-methylpiperazine (54 mg, 0.2 mmol). Purification by preparative HPLC gave **38** as a white TFA salt (23 mg, 16%). ¹H NMR (400 MHz, CD₃OD) δ 7.99 (d, *J* = 8.4 Hz, 1H), 7.71 (d, *J* = 8.0 Hz, 2H), 7.53-7.46 (m, 5H), 7.05 (t, *J* = 7.6 Hz, 1H), 7.04 (d, *J* = 8.0 Hz, 1H), 6.94 (d, *J* = 7.6 Hz, 1H), 6.58 (t, *J* = 7.4 Hz, 1H), 5.99 (d, *J* = 8.0 Hz, 1H), 4.19 (s, 2H), 3.60–3.30 (m, 9H), 2.95 (s, 3H), 2.24 (dd, *J* = 7.6, 4.8 Hz, 1H), 2.18 (dd, *J* = 9.0, 4.6 Hz, 1H); HRMS (ESI) *m/z* calcd for [C₃₁H₃₁N₅O + H]⁺ 490.2607; found, 490.2610; HPLC purity: 99% at 254 nM.

(1*R,2*S**)-2-(3-(4-((diethylamino)methyl)styryl)-1*H*-indazol-6-yl)spiro-[cyclopropane-1,3'-**

indolin]-2'-one (39) The title compound was synthesized according to general procedure C, using **20a** (70 mg, 0.17 mmol) and (*E*)-*N*-ethyl-*N*-(4-(2-(4,4,5,5-tetramethyl-1,3,2-dioxaborolan-2-yl)vinyl)benzyl)ethanamine (68 mg, 0.22 mmol). Purification by preparative HPLC gave **39** as a cream TFA salt (29 mg, 29%). ¹H NMR (400 MHz, CD₃OD) δ 8.01 (d, *J* = 8.4 Hz, 1H), 7.76 (d, *J* = 8.0 Hz, 2H), 7.56–7.52 (m, 4H), 7.48 (s, 1H), 7.04 (d, *J* = 7.2 Hz, 2H), 6.93 (d, *J* = 7.6 Hz, 1H), 6.58 (t, *J* = 7.2 Hz, 1H), 5.98 (d, *J* = 7.6 Hz, 1H), 4.36 (s, 2H), 3.29–3.17 (m, 5H), 2.25 (t, *J* = 4.8 Hz, 1H), 2.21–2.17 (m, 1H), 1.37 (t, *J* = 7.2 Hz, 6H); HRMS (ESI) *m/z* calcd for [C₃₀H₃₀N₄O + H]⁺ 463.2498; found, 463.2491; HPLC purity: >99% at 254 nM.

(1*R,2*S**)-(*E*)-2-(3-(4-(pyrrolidin-1-ylmethyl)styryl)-1*H*-indazol-6-yl)spiro[cyclopropane-1,3'-**

indolin]-2'-one (40) To a solution of **23** (70 mg, 0.17 mmol) and pyrrolidine (71 μL, 0.86 mmol) in THF (3 mL) was added Ti(*i*-OPr)₄ (97 mg, 0.34 mmol) and the mixture was stirred for 30 min. NaBH₄ (13 mg, 0.34 mmol) was added and the mixture was heated to 50 °C overnight. Water (10 mL) was added and the solution was extracted with EtOAc (2 x 10 mL), dried over MgSO₄ and concentrated to a brown solid. Purification by reverse phase preparatory HPLC gave the title compound as a yellow TFA salt (34 mg, 35%). ¹H NMR (400 MHz, CD₃OD) δ 8.02 (d, *J* = 8.6 Hz, 1H), 7.76 (d, *J* = 8.6 Hz, 2H),

7.55–7.48 (m, 5H), 7.08–7.05 (m, 2H), 6.94 (d, $J = 7.8$ Hz, 1H), 6.59 (t, $J = 7.5$ Hz, 1H), 5.99 (d, $J = 7.5$ Hz, 1H) 4.40 (s, 2H), 3.55–3.46 (m, 2H), 3.38–3.34 (m, 1H), 3.27–3.16 (m, 2H), 2.27–2.17 (m, 4H), 2.06–1.98 (m, 2H); HRMS (ESI) m/z calcd for $[C_{30}H_{28}N_4O + H]^+$ 461.2341; found, 461.3336; HPLC purity: 98.9% at 214 nM.

(1*R,2*S**)-(*E*)-2-(3-(4-(piperidin-1-ylmethyl)styryl)-1*H*-indazol-6-yl)spiro[cyclopropane-1,3'-indolin]-2'-one (41)** To a solution of **23** (20 mg, 0.05 mmol) and piperidine (38 μ L, 0.25 mmol) in THF (1 mL) was added $Ti(iOPr)_4$ (28 mg, 0.1 mmol) and the mixture was stirred for 30 min. $NaBH_4$ (4 mg, 0.1 mmol) was added and the mixture was heated to 50 °C overnight. Water (5 mL) was added and the solution was extracted with EtOAc (2 x 10 mL), dried over $MgSO_4$ and concentrated to a yellow oil. Purification by reverse phase preparatory HPLC gave the title compound as a yellow TFA salt (8 mg, 28%). 1H NMR (400 MHz, CD_3OD) δ 8.02 (d, $J = 8.8$ Hz, 1H), 7.77 (d, $J = 8.6$ Hz, 2H), 7.75–7.48 (m, 5H), 7.08–7.05 (m, 2H), 6.94 (d, $J = 7.5$ Hz, 1H), 6.59 (t, $J = 7.7$ Hz, 1H), 5.99 (d, $J = 7.3$ Hz, 1H), 4.31 (s, 2H), 3.53–3.45 (m, 2H), 3.39–3.34 (m, 1H), 3.04–2.93 (m, 2H) 2.27–2.17 (m, 2H), 2.02–1.95 (m, 2H), 1.88–1.71 (m, 3H), 1.57–1.45 (m, 1H); HRMS (ESI) m/z calcd for $[C_{31}H_{30}N_4O + H]^+$ 475.2498; found, 475.2501; HPLC purity: 95.3% at 214 nM.

ASSOCIATED CONTENT:

Supporting Information: Synthesis of compound intermediates; Crystallographic Data and Refinement Statistics for PLK4/compound **18** complex. This material is available free of charge via the Internet at <http://pubs.acs.org>.

ACKNOWLEDGMENT:

We thank Dr. Homer Pearce for helpful discussion during the course of the work. The Princess Margaret Cancer Foundation and the Canadian Foundation for Innovation are acknowledged for financial support.

ABBREVIATIONS USED:

ADME, absorption, distribution, metabolism, excretion; ATP, Adenosine-5'-triphosphate; b, broad; calcd, calculated; CYP; Cytochrome P450; d, doublet; DCM, dichloromethane; DIPEA, diisopropylethylamine; DMF, N,N-dimethylformamide; DMSO, dimethyl sulfoxide; FLT3, fms-related tyrosine kinase 3; GI₅₀, half maximal cell growth inhibitory concentration; G6PDH, glucose-6-phosphate dehydrogenase; GST, Glutathione S-transferase; h, hour; HEPES, 4-(2-hydroxyethyl)-1-piperazineethanesulfonic acid; HPLC, high performance liquid chromatography; IPTG, isopropyl β-D-1-thiogalactopyranoside; IP, intraperitoneal; KD, kinase domain; KDR, kinase insert domain receptor; LCMS, liquid chromatography coupled to mass spectrometry; MBP, Myelin basic protein; min, minute; m, multiplet; MS ESI, Electrospray Ionization mass spectrometry; ND, not determined; NMR, nuclear magnetic resonance; NOE, Nuclear Overhauser effect; PBS, Phosphate Buffered Saline; PDB, protein data bank; PEG400, polyethylene glycol 400; pin, pinacol; PMH, Princess Margaret Hospital; PPB, Plasma Protein Binding; prep, preparative; QD, once a day; RBF, round bottomed flask; RMSE root-mean-square deviation; rt, room temperature; RP, reverse phase; s, singlet; SAR, structure-activity relationship; satd, saturated; SEM, 2-(Trimethylsilyl)ethoxy]methyl; SFC, super-critical fluid chromatography; SRB, sulforhodamine B; SUMO, small ubiquitin modifier; t, triplet; TEA, triethylamine; temp, temperature; TFA, trifluoroacetic acid; TGI, tumor growth inhibition; THF, tetrahydrofuran; TLC, thin layer chromatography; tol, toluene; q, quartet; UHN IACUC, University Health Network Institutional Animal Care and Use Committee.

AUTHOR INFORMATION:

Corresponding Author: Peter B. Sampson

*Phone: 416-581-7724. E-mail: psampson@uhnresearch.ca;

1
2 REFERENCES:
3
4
5

6 (1) Jackson, J.R.; Patrick, D.R.; Dar, M.M.; Huang, P.S.; Targeted anti-mitotic therapies: can we
7 improve on tubulin agents? *Nat. Rev. Cancer* **2007**, *7*, 107–117.
8

9
10
11 (2) Schmidt, M.; Bastians, H.; Mitotic drug targets and the development of novel anti-mitotic anticancer
12 drugs. *Drug Res. Updates*, **2007**, *10*, 162–181.
13
14
15
16

17
18
19 (3) Matthews, N.; Visintin, C.; Hartzoulakis, B.; Jarvis, A.; Selwood, D.L. Aurora A and B kinases as
20 targets for cancer: will they be selective for tumors? *Expert Rev. Anticancer Ther.* **2006**, *6*, 109–120.
21
22
23
24

25 (4) Kollareddy, M.; Zheleva, D.; Dzubak, P.; Brahmshatriya, P.S.; Lepsik, M.; Hajduch, M.; Aurora
26 kinase inhibitors: progress towards the clinic. *Invest. New Drugs* **2012**, *31*, 2411–2432.
27
28
29
30

31
32 (5) Friedberg, J.W.; Mahadevan, D.; Cebula, E.; Persky, D.; Lossos, I.; Agarwal, A.B.; Jung, J.; Burack,
33 R.; Zhou, X.; Leonard, E.J.; Fingert, H.; Danaee, H.; Bernstein, S.H. Phase II Study of Alisertib, a
34 selective Aurora A kinase inhibitor, in relapsed and refractory aggressive B- and T-Cell non-Hodgkin
35 lymphomas. *J. Clin. Oncol.* **2014**, *32*, 44–50.
36
37
38
39
40

41
42
43 (6) Barr, F.A.; Silljé, H.H.W.; Nigg, E.A.; Polo-like kinases and the orchestration of cell division. *Nat.*
44 *Rev. Mod. Cell* **2004**, *5*, 429–440.
45
46
47
48

49 (7) Eckerdt, F.; Yuan, J.; Strebhardt, K. Polo-like kinases and oncogenesis. *Oncogene* **2005**, *24*, 267–
50 276.
51
52
53
54
55
56
57
58
59
60

- 1
2 (8) Johnson, E.F.; Stewart, K.D.; Woods, K.W.; Giranda, V.L.; Luo, Y. Pharmacological and functional
3 comparison of the polo-like kinase family: Insight into inhibitor and substrate specificity. *Biochemistry*
4 **2007**, *46*, 9551–9563.
5
6
7
8
9
10 (9) Lens, S.M.A.; Voest, E.E.; Medema, R.H. Shared and separate functions of polo-like kinases and
11 aurora kinases in cancer. *Nat. Rev. Cancer* **2010**, *10*, 825–841.
12
13
14
15
16 (10) Schoffski, P.; Polo-like kinase inhibitors in preclinical and early clinical development. *Oncologist*
17 **2009**, *14*, 559–570.
18
19
20
21
22 (11) Frost, A.; Kross, K.; Steinbild, S.; Hedbom, S.; Unger, C.; Kaiser, R.; Trommeshauser, D.;
23 Munzert, G. Phase I study of the PLK1 inhibitor BI 2536 administered intravenously on three
24 consecutive days in advance solid tumours. *Curr. Oncol*, **2012**, *19*, 28–35.
25
26
27
28
29
30
31 (12) Leung, G.C.; Hudson, J.W.; Kozarova, A.; Davidson, A.; Dennis, J.W.; Sicheri, F. The Sak polo-
32 box comprises a structural domain sufficient for mitotic subcellular localization. *Nat. Structural Biol.*
33 **2002**, *9*, 719–724.
34
35
36
37
38
39 (13) Sillibourne, J.E.; Bornens, M.; Polo-like kinase 4: the odd one out of the family. *Cell Div.* **2010**, *5*,
40 25–34.
41
42
43
44
45 (14) Bettencourt-Dias, M.; Rodrigues-Martins, A.; Carpenter, L.; Riparbelli, M.; Lehmann, L.; Gatt,
46 M.K.; Carmo, N.; Balloux, F.; Callani, G.; Glover, D.M. SAK/PLK4 is required for centriole
47 duplication and flagella development. *Curr. Biol.* **2005**, *15*, 2199–2207.
48
49
50
51
52 (15) Habedanck, R.; Stierhof, Y-D.; Wilkinson, C.J.; Nigg, E.A. The Polo kinase PLK4 functions in
53 centriole duplication. *Nat. Cell Biol.* **2005**, *7*, 1140–1146.
54
55
56
57
58
59
60

1
2 (16) Mason, J.; Wei, S.; Luo, S.; Nadeem, V.; Kiarash, R.; Huang, P.; Awrey, A.; Leung, G.;
3
4 Beletskaya, I.; Feher, M.; Forrest, B.; Laufer, R.; Sampson, P.; Li, S-W.; Liu, Y.; Lang, Y.; Pauls,
5
6 H.W.; Mak, T.W.; Pan, J. G. Inhibition of Polo-like kinase 4 as an anti-cancer strategy, *Book of*
7
8 *Abstracts*, AACR 102nd Annual Meeting, Orlando, FL, Apr. 2-6, 2011., LB-215.

9
10
11
12
13
14 (17) Mak, T.W. Targeting the cell cycle in cancer: TTK (MPS1) and PLK4 as novel mitotic targets,
15
16 *Book of Abstracts*, AACR 103rd Annual Meeting, Chicago, IL, Apr. 1-5, 2012.

17
18
19
20
21 (18) Pauls, H.W. The discovery of PLK4 inhibitors as novel antiproliferative agents, *Book of Abstracts*,
22
23 Canadian Chemistry Conference & Exhibition, Quebec City, QC, May 26-29 (2013), BM7-00029.

24
25
26
27 (19) Laufer, R.; Forrest, B.; Li, S.; Sampson, P.; Liu, Y.; Edwards, L.; Lang, Y.; Awrey, D.; Mao, G.;
28
29 Plotnikova, O.; Leung, G.; Hodgson, R.; Beletskaya, I.; Mason, J.; Luo, X.; Nadeem, V.; Feher, M.;
30
31 Ban, F.; Wei, S.; Kiarash, R.; Green, E.; Mak, T.; Pan, J.; Pauls, H.W. The discovery of PLK4
32
33 inhibitors: (*E*)-3-((1H-indazol-6-yl)methylene)indolin-2-ones as novel anti-proliferative agents. *J. Med.*
34
35 *Chem.* **2013**, *56*, 6069–6087.

36
37
38
39
40 (20) Harrington, E.A.; Bebbington, D.; Moore, J.; Rasmussen, R.K.; Ajose-Adeogun, A.O.; Nakayama,
41
42 T.; Graham, J.A.; Demur, C.; Hercend, T.; Diu-Hercend, A.; Su, M.; Golec, J.M.C.; Miller, K.M. VX-
43
44 680, a potent and selective small-molecule inhibitor of the Aurora kinases, suppresses tumor growth *in*
45
46 *vivo*. *Nat. Med.* **2004**, *10*, 262–267.

47
48
49
50
51 (21) Hu-Lowe, D.D.; Zou, H.Y.; Grazzini, M.L.; Hallin, M.E.; Wickman, G.R.; Amundson, K.; Chen,
52
53 J.H.; Rewolinski, D.A.; Yamazaki, S.; Wu, E.Y.; McTigue, M.A.; Murray, B.W.; Kania, R.S.;
54
55 O'Connor, P.; Shalinsky, D.R.; Bender, S.L. Nonclinical antiangiogenesis and antitumor activities of
56
57
58
59
60

1
2 Axitinib (AG-013736), an oral, potent, and selective inhibitor of vascular endothelial growth factor
3
4 receptor tyrosine kinases 1, 2, 3. *Clin Cancer Res* **2008**, *14*, 7272–7283.
5
6

7
8
9 (22) Johnson, E.F.; Stewart, K.D.; Woods, K.W.; Giranda, V.L.; Luo, Y. Pharmacological and
10 functional comparison of the Polo-like kinase family: insight into inhibitor and substrate specificity.
11
12 *Biochemistry*, **2007**, *46*, 9551–9563.
13
14
15

16
17
18 (23) Donaldson, W.A. Synthesis of cyclopropane containing natural products *Tetrahedron*, **2001**, *57*,
19
20 8589–8627.
21
22

23
24 (24) Lebel, H.; Marcoux, J.F.; Molinaro, C.; Charette, A.B. Stereoselective cyclopropanation reactions
25
26 *Chem. Rev.* **2003**, *103*, 977–1050.
27
28

29
30 (25) Reichelt, A.; Martin, S.F. Synthesis and properties of cyclopropane-derived peptidomimetics *Acc.*
31
32 *Chem. Res.* **2006**, *39*, 433–442.
33
34

35
36 (26) Mattson, R.J.; Catt, J.D.; Denhart, D.J.; Deskus, J.A.; Ditta, J.L.; Higgins, M.A.; Marcon, L.R.;
37
38 Sloan, C.P.; Beno, B.R.; Gao, Q.; Cunningham, M.A.; Mattson, G.K.; Molski, T.F.; Taber, M.T.;
39
40 Lodge, N.J. Conformationally restricted homotryptamines. 2. Indole cyclopropylmethylamines as
41
42 selective serotonin reuptake inhibitors. *J. Med. Chem.* **2005**, *48*, 6023–6034.
43
44
45

46
47 (27) Jiang, T.; Kuhen, K.L.; Wolff, K.; Yin, H.; Bieza, K.; Caldwell, J.; Bursulaya, B.; Wub, T.Y.; Hea, Y.
48
49 Design, synthesis and biological evaluations of novel oxindoles as HIV-1 non-nucleoside reverse
50
51 transcriptase inhibitors. Part I. *Bioorg. Med. Chem. Lett.* **2006**, *16*, 2105–2108.
52
53
54

55
56 (28) Wurster, J.A. 3-Spirocyclopropyl-2-oxindole compound tyrosine kinase inhibitors, and their
57
58 therapeutic use. PCT Int. Appl. **2007** WO2007008664.
59
60

- 1
2 (29) Corey, E.J.; Chaykovsky, M. Dimethyloxosulfonium methylide and dimethylsulfonium methylide.
3
4 Formation and application to organic synthesis. *J. Am. Chem. Soc.* **1965**, *87*, 1353–1364.
5
6
7
8 (30) Ciaccio, J.A.; Aman, C.E. “Instant methylide” modification of the Corey-Chaykovsky
9
10 cyclopropanation reaction. *Synth. Commun.* **2006**, *36*, 1333–1341.
11
12
13
14 (31) Moldvai, I.; Gacs-Baitz, E.; Balazs, M.; Incze, M.; Szantay, C. Synthesis of spiro[cyclopropane-
15
16 1,3' [3H]indol]-2' (1'H)-ones with antihypoxic effects. *Arch. Pharm. Pharm. Med. Chem.* **1996**, *329*,
17
18 541–549.
19
20
21
22 (32) Murata, M.; Watanabe, S.; Masuda, Y. Formation of (Z)allylboronates vis ruthenium-catalyzed
23
24 hydroboration of propargyl ethers with pinacalborane. *J. Chem. Research (S)*, **2002**, 142–143.
25
26
27
28
29 (33) Hunt, A.R.; Stewart, S.K.; Whiting, A. Heck versus Suzuki palladium catalyzed cross-coupling of a
30
31 vinylboronate ester with aryl halides. *Tet. Lett.* **1993**, *34*, 3599–3602.
32
33
34
35
36 (34) Usansky, J.I.; Desai, A.; Tang-Liu, D. PK functions for Microsoft Excel.
37
38 <http://www.boomer.org/pkin/soft.html>, Accessed November, 2008.
39
40
41
42 (35) Kabsch, W. XDS. *Acta Crystallogr D Biol Crystallogr* **2010**, *66*, 125–132.
43
44
45
46 (36) Adams, P.; Afonine, P.; Bunkoczi, G. PHENIX: a comprehensive Python-based system for
47
48 macromolecular structure solution. *Acta Crystallogr D Biol Crystallogr* **2010**, *66*, 213–221.
49
50
51
52 (37) Emsley P.; Cowtan K. Coot: model-building tools for molecular graphics. *Acta Crystallogr. D60*,
53
54 **2004**, 2126–2132.
55
56
57
58
59
60

1
2 (38) Bricogne G., B. E., Brandl M., Flensburg C., Keller P., Paciorek W., Roversi P, Sharff A., Smart
3
4 O.S., Vonrhein C., Womack T.O. *Buster 2.10.0*, 2.10.0; Global Phasing Ltd: Cambridge, United
5
6 Kingdom, 2011.
7

8
9
10
11 (39) Schrödinger Suite 2009 Protein Preparation Wizard; Epik version 2.0, Schrödinger, LLC, New
12
13 York, NY, 2009; Impact version 5.5, Schrödinger, LLC, New York, NY, 2009; Prime version 2.1,
14
15 Schrödinger, LLC, New York, NY, 2009.
16

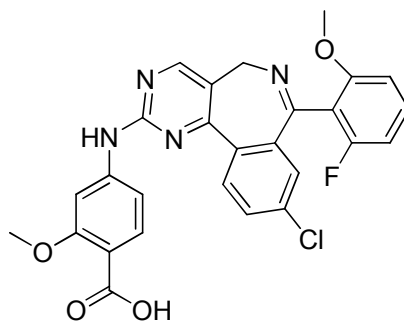
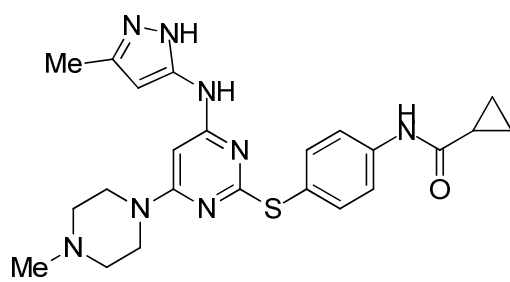
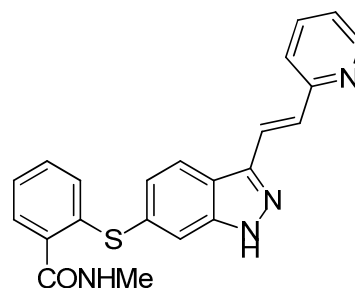
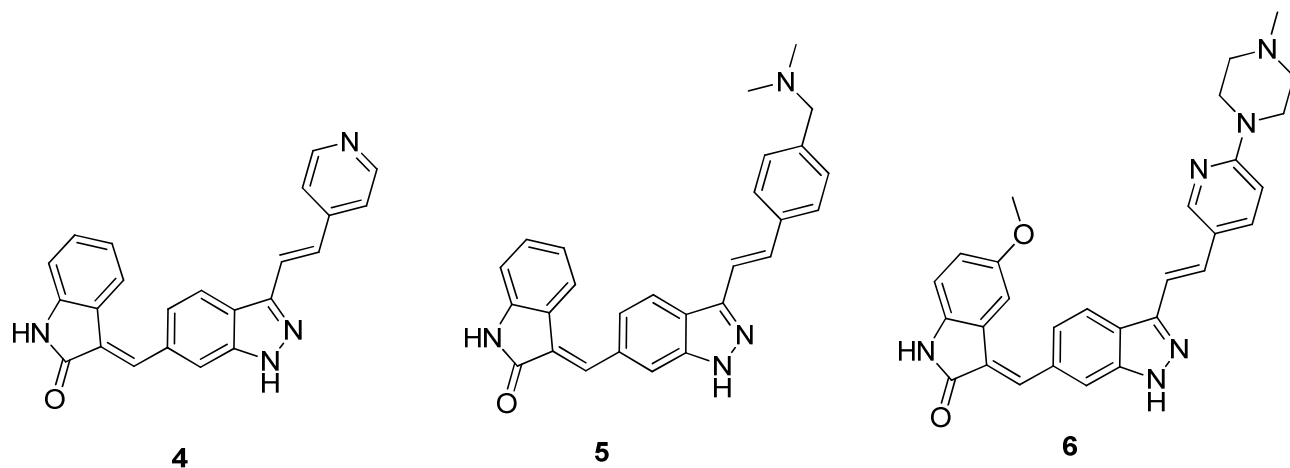
17
18
19 (40) MOE (Molecular Operating Environment) version 2009.10; Chemical Computing Group Inc.: 1010
20
21 Sherbrooke St. West, Suite 910, Montreal, Quebec, H3A 2R7, Canada.
22

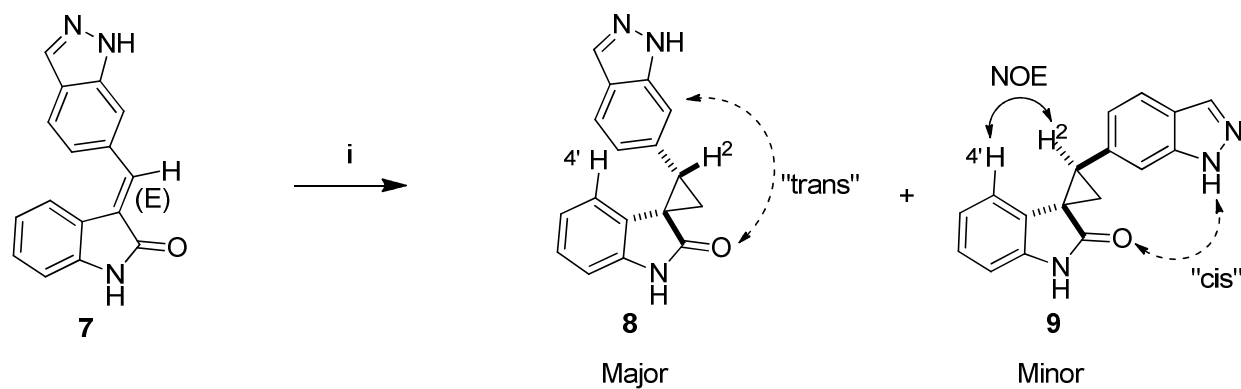
23
24
25 (41) Corina, version 3.2; Molecular Networks GmbH: Erlangen, Germany, 2006.
26

27
28
29 (42) Feher, M; Williams, C.I. Effect of input differences on the results of docking calculations. *J. Chem.*
30
31 *Inf. Model.* **2009**, *49*, 1704–1714.
32

33
34
35 (43) Feher, M.; Williams, C. I. Numerical errors and chaotic behavior in docking simulations. *J. Chem.*
36
37 *Inf. Model.* **2012**, *52*, 724–738.
38

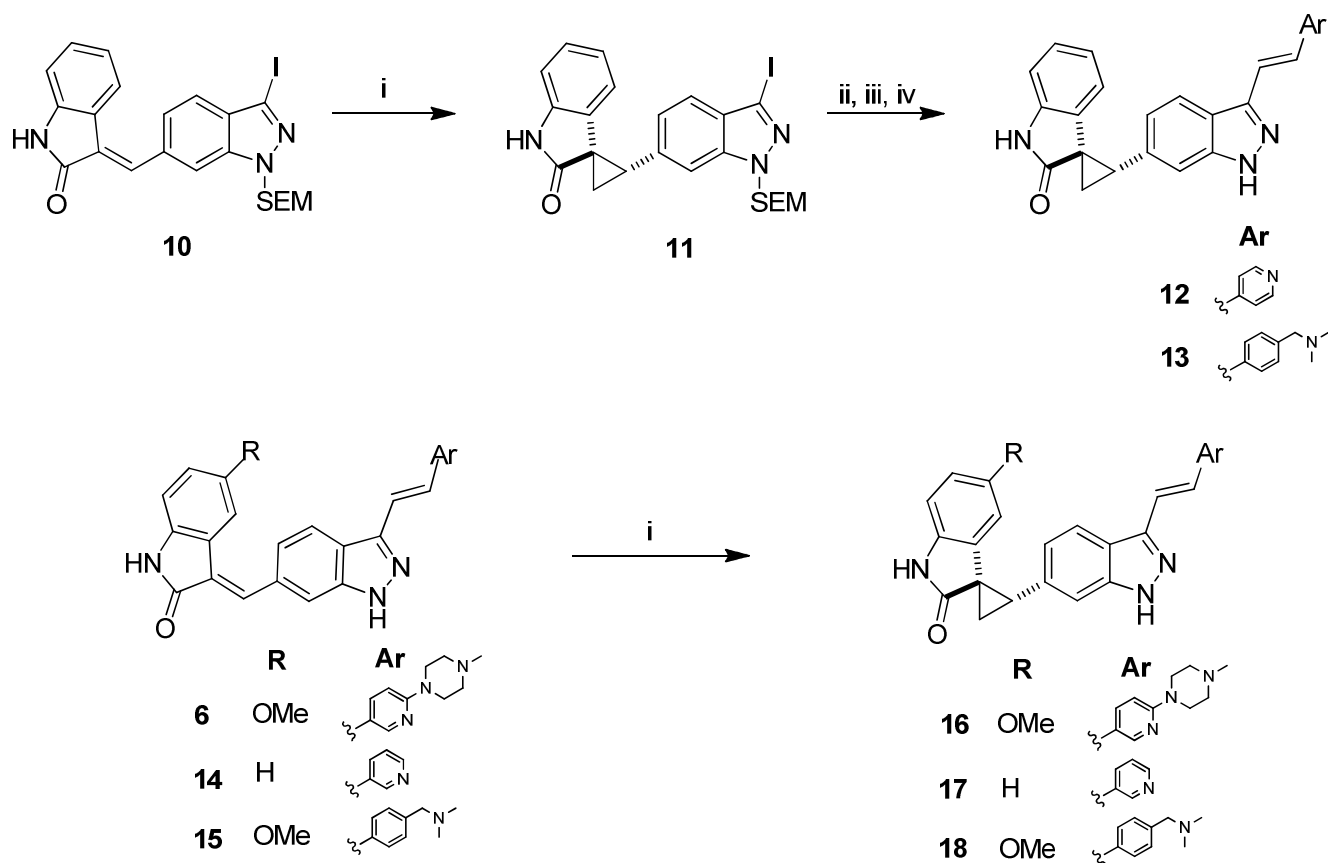
39
40
41 (44) Glide, version 2009; Schrodinger Inc.: Portland, OR, USA, 2007.
42
43
44
45
46
47
48
49
50
51
52
53
54
55
56
57
58
59
60

**1 Alisertib****2, VX-680, PLK4 Ki = 11 nM****3, Axitinib, PLK4 Ki = 4.2 nM****Figure 1. PLK4 Activity of Known Kinase Inhibitors****Figure 2. (E)-3-((1H-indazol-6-yl)methylene)indolin-2-one PLK4 Inhibitors****Scheme 1. Synthesis of racemic 2-(1H-indazol-6-yl)spiro[cyclopropane-1,3'-indolin]-2'-ones**



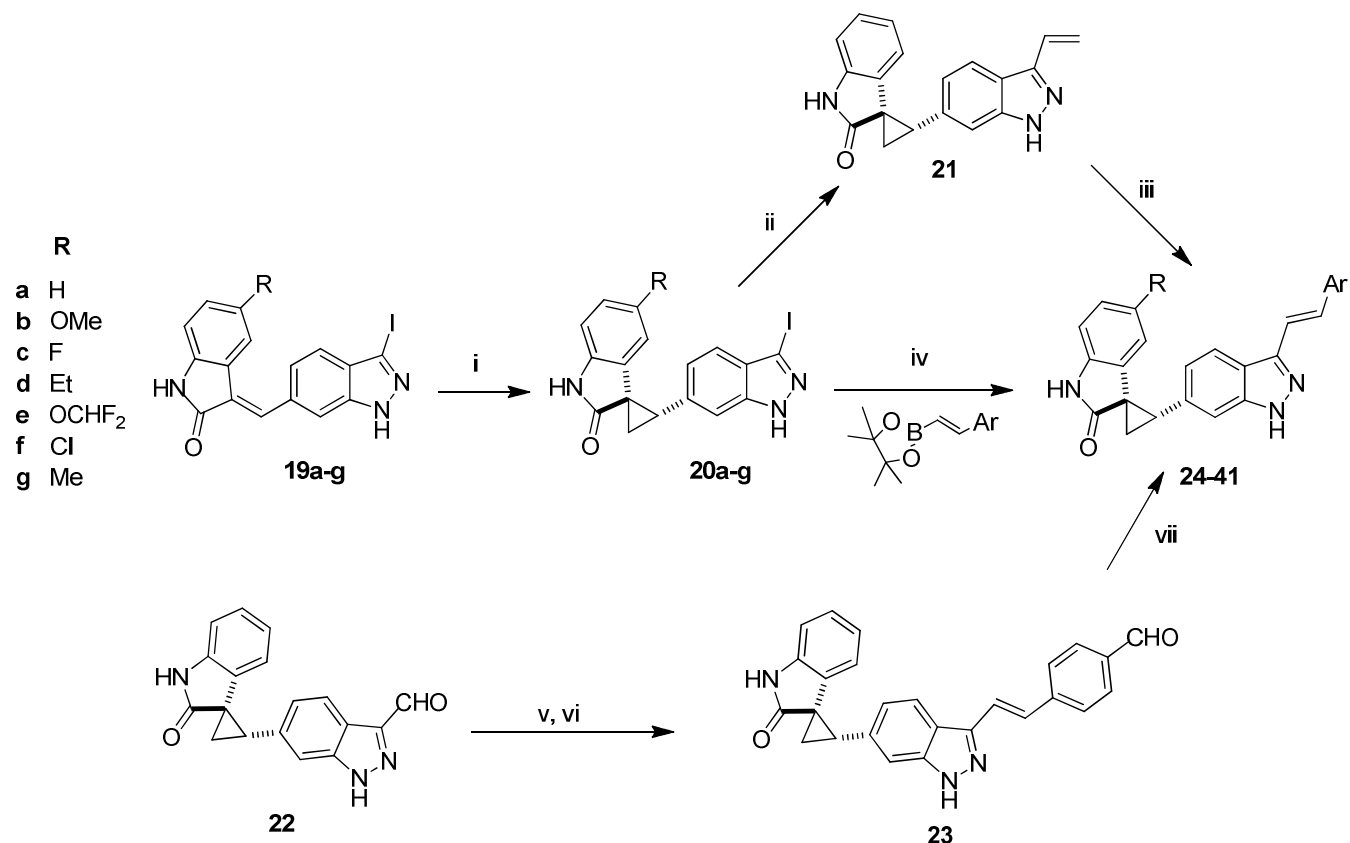
Reagents and Conditions: (i) Me₃SOI, NaH, DMF, rt

Scheme 2. Synthesis of racemic vinylaryl 2-(1H-indazol-6-yl)spiro[cyclopropane-1,3'-indolin]-2'-ones by cyclopropanation of methylene-indolin-2-one



Reagents and Conditions: (i) Me_3SOI , NaH, DMF, rt; (ii) $\text{ArCH}=\text{CH}_2$, 5 mol% $\text{Pd}(\text{OAc})_2$, $\text{P}(\text{oTol})_3$, DIPEA, DMF, 130 °C, 2h; (iii) BF_3OEt_2 , CH_2Cl_2 , 2 h; (iv) 2:1 EtOH/2 M aq. HCl, 50 °C, 2 h.

Scheme 3. Synthesis of racemic vinylaryl 2-(1H-indazol-6-yl)spiro[cyclopropane-1,3'-indolin]-2'-ones



Reagents and Conditions: (i) Me₃SOI, NaH, DMF, rt; (ii) 4,4,5,5-tetramethyl-2-vinyl-1,3,2-dioxaborolane, 2 mol% Pd(PPh₃)₄, 2:1 PhCH₃/EtOH, 1 M aq. Na₂CO₃, 125 °C, 3 h; (iii) ArBr, 5 mol% Pd(OAc)₂, P(o-tol)₃, DIPEA, DMF, 125 °C, 2 h; (iv) 3:1 EtOH/PhCH₃, 1 M aq. Na₂CO₃, Pd(PPh₃)₄, 120 °C, 2 h; v) diethyl 4-cyanobenzylphosphonate, t-BuOK, DMF, 0 °C; vi) Raney Nickel, NaH₂PO₂, DMF, pyridine, AcOH, H₂O, 60 °C; vii) R'₂NH, Ti(Oi-Pr)₄, NaBH₄, THF, 40 °C.

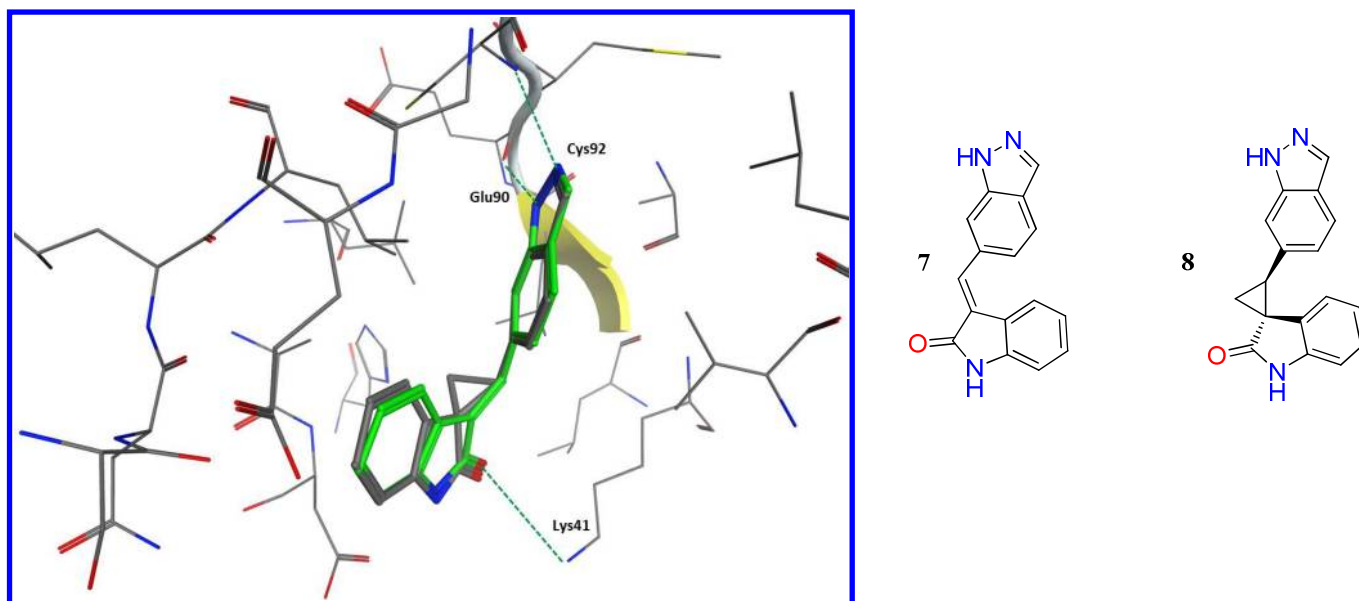


Figure 3. Comparison of *E*-alkene **7** (green) and the (1*R*,2*S*)-cyclopropane **8** (grey) bioisosteres in the PLK4 binding site. This view was generated by GlideXP docking into the 3COK-based model.

Table 1. Effect of Alkene to Cyclopropane Bioisosteric Replacement on Kinase and CYP450 Inhibition.

Compound	Kinase IC ₅₀ (μM)			CYP450 Enzyme IC ₅₀ (μM)				
	PLK4	FLT3	KDR	1A2	2C9	2C19	2D6	3A4
(<i>E</i>)-3-((1<i>H</i>-indazol-6-yl)methylene)indolin-2-one								
7	0.23	0.14	2.5	0.050	0.5	0.21	>1.0	~10
4	0.0024	0.035	0.034	>10	0.02	0.13	20	1
5	0.004	0.035	0.022	>10	1.4	1.0	8.9	0.94
6	0.0004	0.18	0.48	>10	1.6	0.8	>10	>1
(2-(1<i>H</i>-indazol-6-yl)spiro[cyclopropane-1,3'-indolin]-2'-one)^a								
8	1.0	3.2	>10	>10	>10	~10	>10	>10
9	> 50	ND	ND	ND	ND	ND	ND	ND
12	0.0036	0.033	1.3	1.4	0.03	0.26	0.7	>1
13	0.0018	0.011	0.11	>10	>1	>1	3.1	>10
16	0.0018	0.024	2.0	>10	1.6	1.6	>10	2.1

a) Racemic mixture

Table 2. Effect of Alkene to Cyclopropane Bioisosteric Replacement on Cell Activity, Solubility and ADME Properties.

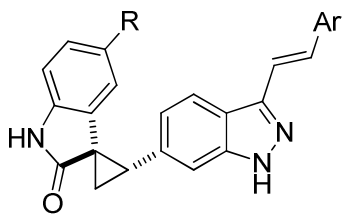
Entry	Cancer Cell Line GI ₅₀ (μM)		Sol. @ pH 7.4 (μg/ml)	PPB %	Microsomal t _{1/2} (min)		IP Mouse Plasma Levels (50 mg/kg)	
	MCF-7	MDA- MB-468			mouse	human	C _{max} (μg/ml)	AUC (μg.hr/ml)
(E)-3-((1H-indazol-6-yl)methylene)indolin-2-one								
7	5.3	4.6	0.7	>99.9	5	54	0.011	0.061
4	0.16	0.31	0.21	98.9	6	29	<0.01	ND
5	0.007	0.012	<0.1	98.4	7	40	0.87	0.83
6	<0.01	<0.01	<0.1	99.1	2	14	0.09	0.19
2-(1H-indazol-6-yl)spiro[cyclopropane-1,3'-indolin]-2'-one^a								
8	16	14	8.0	83	49	>60	1.20	1.62
12	0.51	0.36	0.4	95.5	18	>60	1.7	2.9
13	<0.01	<0.01	1.7	94.7	13	>60	2.6	7.2
16	0.04	<0.01	0.19	ND	9	16	0.20	0.45

a) Racemic mixture

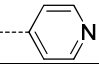
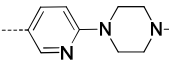
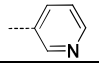
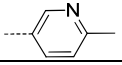
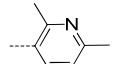
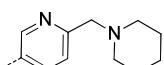
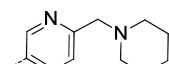
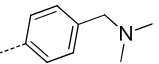
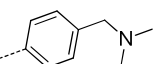
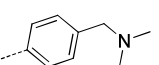
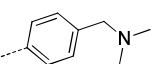
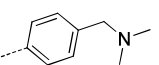
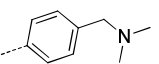
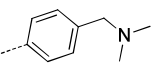
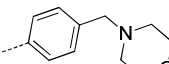
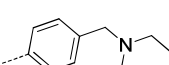
Table 3. Polo-like Kinase Activity of Alkene and Racemic Cyclopropane Compounds

Entry	IC ₅₀ (nM)			
	PLK4	PLK1	PLK2	PLK3
4	2.4	>10 ⁵	>10 ⁵	>10 ⁵
12	3.6	>10 ⁵	>10 ⁵	>10 ⁵
13	1.6	>10 ⁵	>10 ⁵	>10 ⁵

**Table 4. In Vitro Activity of Racemic 2-(1H-indazol-6-yl)spiro[cyclopropane-1,3'-indolin]-2'-one
PLK4 Inhibitors**



1
2
3
4
5
6
7
8
9
10
11
12
13
14
15
16
17
18
19
20
21
22
23
24
25
26
27
28
29
30
31
32
33
34
35
36
37
38
39
40
41
42
43
44
45
46
47
48
49
50
51
52
53
54
55
56
57
58
59
60

Entry	Ar	R	PLK4 IC ₅₀ (nM)	GI ₅₀ (μM)			
				MCF-7	MDA- MB-468	MDA- MB-231	SKBr-3
3			43	2.3	2.8	11	4.6
4			2.4	0.16	0.31	19	25
6			7.3	<0.01	<0.01	<0.01	2.3
12		H	3.6	0.6	0.36	0.68	20.3
16		OMe	2.2	0.01	0.006	0.01	13.4
17		H	1.6	3.6	0.009	50	14.7
24		H	4.6	0.28	0.14	3.8	7.6
25		H	6.3	6.8	0.07	>50	50
26		H	2.0	1x10 ⁻⁵	4x10 ⁻⁴	35.8	3.4
27		OMe	1.4	1x10 ⁻⁵	2x10 ⁻⁵	3.9	9.2
13		H	1.4	<0.01	<0.01	<0.01	17.8
18		OMe	1.1	<0.001	0.01	<0.01	6.4
28		OCHF ₂	2.6	0.025	0.005	4.8	1.6
29		Cl	1.2	1x10 ⁻⁵	6x10 ⁻⁵	0.93	3.5
30		Me	0.71	1x10 ⁻⁵	5x10 ⁻⁵	2.8	3.4
31		F	0.79	0.1	0.01	0.55	2.2
32		Et	2.0	0.24	0.01	2.0	2.0
33		H	2.3	0.01	0.01	<0.01	11.3
34		OMe	2.2	<0.01	<0.01	<0.01	13.8

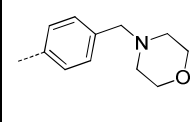
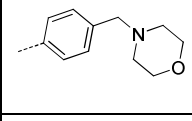
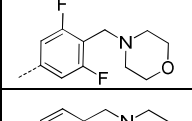
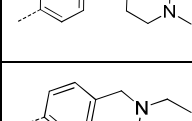
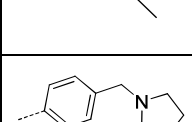
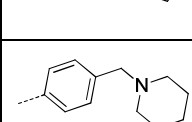

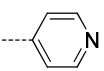
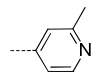
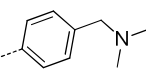
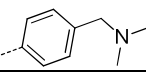
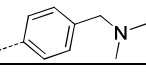
35		F	4.9	0.9	0.02	0.72	10
36		Me	7.2	0.08	0.03	0.56	8.8
37		OMe	3.4	0.05	0.06	1.7	3.7
38		H	2.4	0.01	0.01	2.5	6.0
39		H	1.8	0.11	<0.01	1.7	4.3
40		H	1.3	0.05	<0.01	1.9	4.1
41		H	6.7	0.6	0.5	0.9	0.8

Table 5. Kinase Selectivity of Racemic 2-(1H-indazol-6-yl)spiro[cyclopropane-1,3'-indolin]-2'-one PLK4 Inhibitors.

Entry	Ar	R	IC ₅₀ (nM)			
			PLK4	KDR	AURKB	Flt3
4			2.4	34	24	35
12		H	3.6	1300	7.4	33
25		H	6.3	2100	10	59
13		H	1.4	200	6.4	11
18		OMe	1.1	910	15	19
28		OCHF ₂	2.6	4900	33	32

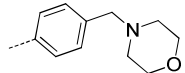
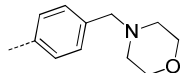
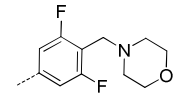
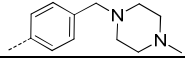
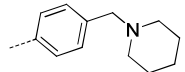
33		H	2.3	1400	49	93
34		OMe	2.2	24,000	29	65
37		OMe	3.4	7900	51	150
38		H	2.4	120	180	120
41		H	6.7	12	14	15

Table 6. Mouse Plasma Exposure and Cytochrome P450 Profile of PLK4 inhibitors

Entry	Mouse Plasma (Oral, 25mg/kg)		P450 Enzyme IC ₅₀ (μM)				
	C _{max} (ng/ml)	AUC (ng·hr/ml)	2C9	2C19	1A2	3A4	2D6
12	470	650	0.03	0.26	1.4	>10	0.7
17	37	93	0.32	0.11	0.14	>1	>1
27	290	740	1.4	0.6	ND	ND	ND
13	290	310	>1	>1	>10	>10	3.6
18	350	730	0.85	0.75	>10	>1	>10
33	1800	4300	1.4	1.8	>10	>1	>10
34	1700	4900	1.4	2.1	>10	>1	>1
35	3700	7940	0.5	1.0	>10	>1	>10
38	190	580	>1	>1	>1	>10	>10

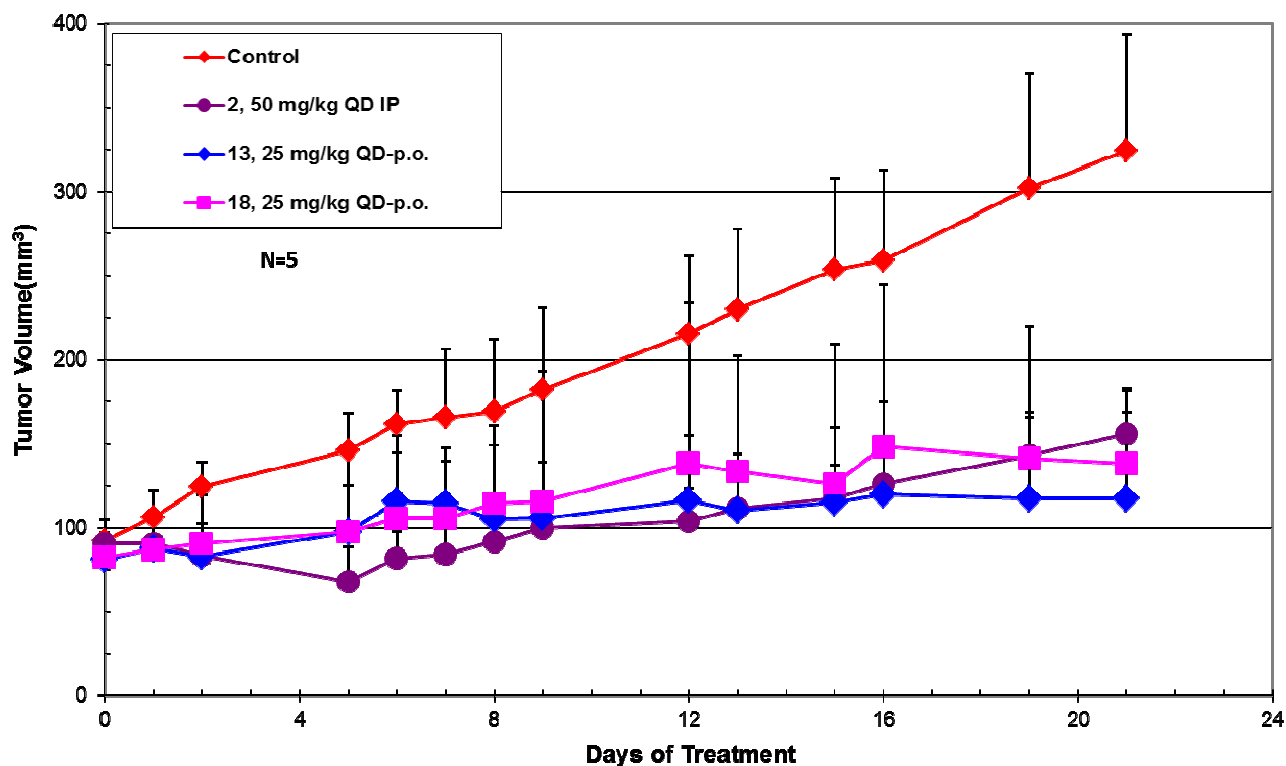
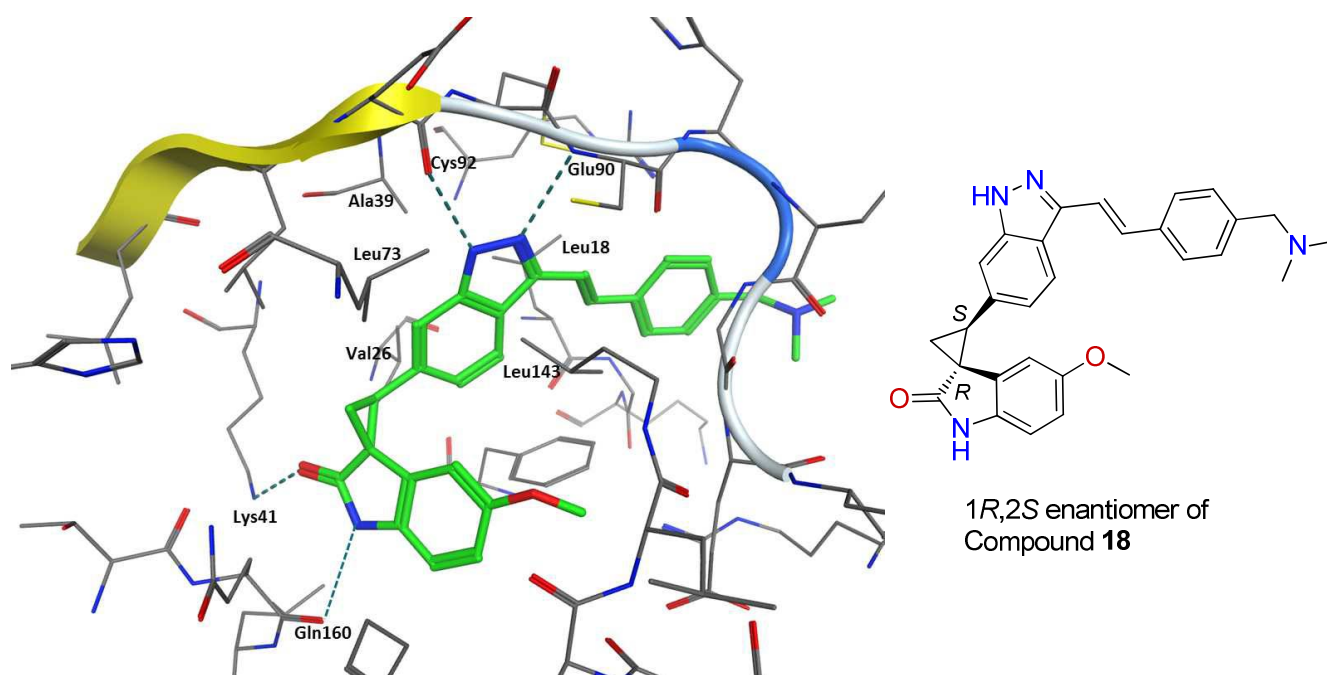
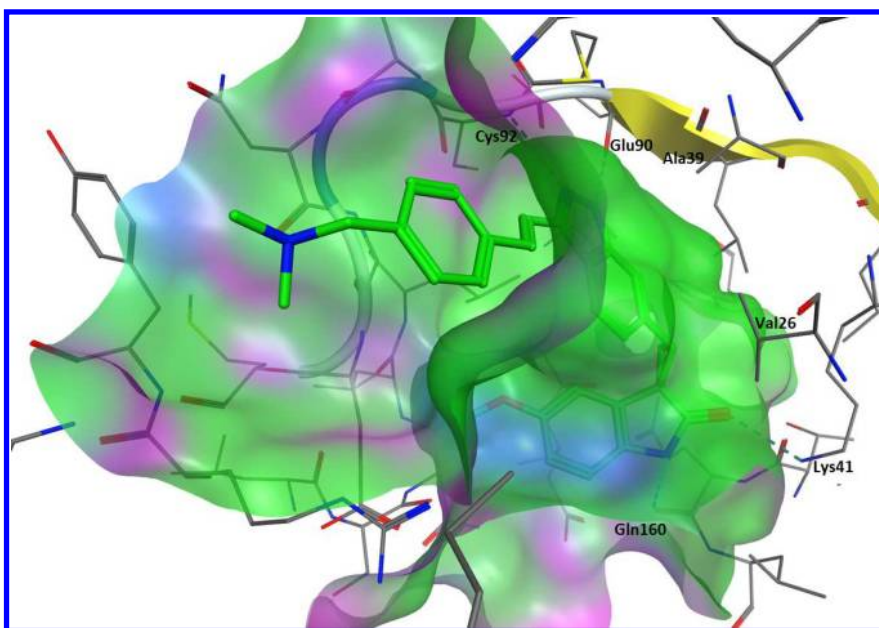


Figure 4. Comparison of in vivo efficacy of PLK4 inhibitors in a mouse MDA-MB-468 breast cancer xenograft model after 21-day treatment (n = 5). **2**, TGI = 73%, p = 0.036; compound **13**, TGI = 84%, p = 0.03; compound **18**, TGI = 76%, p = 0.03. No animals were lost during the course of the study and weight loss was < 20% for all treatment arms; TGI, tumor growth inhibition.

A)



B)



24
25
26
27
28
29
30
31
32
33
34
35
36
37
38
39
40
41
42
43
44
45
46
47
48
49
50
51
52
53
54
55
56
57
58
59
60

Figure 5. X-ray structure of the active site of the PLK4 enzyme at 2.4 Å resolution (PDB code: 4JXF), co-crystallized with racemic compound **18**. The co-structure clearly shows binding of the 1R,2S enantiomer of compound **18**. Hydrogen bonds are depicted by dashed lines. (A) Hydrogen bonding of the indazole to Glu90 and Cys 92 of the hinge region; H-bonds from the indolinone moiety to the sidechain of Lys41 and the backbone carbonyl of Gln160. (B) 180° flipped view of PLK4 active site

1 surface: the dimethylamino group extends into solvent; hydrophobic surfaces engage the indazole and
2 vinyl groups.
3
4
5
6

7 Table of Contents Graphic:
8
9

